https://doi.org/10.5194/egusphere-2026-2711
Preprint. Discussion started: 22 May 2026

Hydrological spatial coupling within an abandoned Mediterranean terraced microcatchment

Jaume Company[1], Francisco Cuello-Llobell[1], Julián García-Comendador[1], Josep Fortesa[1], Miquel Tomàs-Burguera[1], Miquel Mir-Gual[1], Laura Turnbull[2], John Wainwright[2], Mariano Moreno-de-las-Heras[3], Jordi Cristóbal[4], Adolfo Calvo-Cases[5], Joan Estrany[1]

[1]Natural Risks and Emergencies Observatory of the Balearic Islands—RiscBal; https://riscbal.uib.eu/, University of the Balearic Islands. Department of Geography and Institute of Agro-Environmental & Water Economy Research—INAGEA; Centre Bit Raiguer, Carrer dels Selleters 25, 07300 Inca, Mallorca – Spain

[2]Department of Geography, Durham University, Durham, United Kingdom

[3]Grupo de Investigaciones Ambientales Mediterráneas (GRAM), Department of Geography, University of Barcelona, Barcelona, Spain

[4]Department of Geography, Universitat Autònoma de Barcelona, Campus de Bellaterra, Edifici B, Carrer de la Fortuna, s/n, 08193 Bellaterra, Spain

[5]Inter-University Institute for Local Development, Universitat de València, València, Spain

Correspondence to: Jaume Company (jaume.company@uib.eu)

Abstract. Runoff (R) generation in Mediterranean headwater catchments is highly episodic and shaped by the interplay of precipitation (P), seasonal soil moisture (SM) dynamics, and terrain structure. In terraced landscapes, land abandonment has driven a forest transition that increases fuel loads and wildfire occurrence, while legacy features such as stone walls modify storage and flow pathways, affecting hydrological spatial coupling. Wildfires further reduce vegetation cover, induce soil water repellence, and lower infiltration capacity, enhancing R generation and reorganising connectivity during a post-fire window of disturbance, but their interaction with terrace structure at event scale is poorly understood. This study investigates how P, seasonal evolving SM, and terrain structure control R in a 4.7 ha terraced microcatchment in Mallorca, Spain, affected by a high-severity wildfire in 2013. Hydrological conditions were classified into four periods (wet, drying-down, dry, and wetting-up). P, SM, and discharge (Q) were continuously monitored over four years (2021-2024), with SM measured at representative hillslope and terrace locations. Of 186 P events analyzed, only 17 % generated measurable outlet Q, with R highly concentrated in time: November 2021 alone accounted for 73 % of total R volume. Maximum SM consistently emerged as the strongest indicator of R occurrence across seasons, while event-scale changes in SM (ΔSM) were particularly informative during transitional periods; antecedent SM showed limited predictive power, especially under partially coupled conditions. Hillslopes responded rapidly to P but with weak coupling between local SM and outlet Q, whereas farm terraces exhibited storage-controlled behaviour in well-connected positions and delayed or suppressed responses in disconnected mid-terrace areas. Overall, R emerges from the interaction between P forcing, dynamically evolving SM, and spatially variable structural

https://doi.org/10.5194/egusphere-2026-2711
Preprint. Discussion started: 22 May 2026

connectivity, rather than from static thresholds, highlighting the need for connectivity-aware, event-scale approaches to inform land management in Mediterranean landscapes under global change.

1 Introduction

Runoff (R) response in Mediterranean headwater catchments is highly episodic and characterized by strong temporal variability, with a small number of precipitation (P) events contributing disproportionately to total R (Gallart et al., 2002; García-Comendador et al., 2017; Licciardello et al., 2019). This behaviour reflects the combined influence of climatic forcing and internal catchment state, particularly soil moisture (SM), which regulates whether hydrological pathways become effectively connected and able to transmit flow to the outlet (McDonnell et al., 2021; Penna et al., 2011). In this context, hydrological coupling describes the degree to which spatially distributed hydrological responses become connected and integrated across the catchment, enabling locally generated flows to propagate towards the outlet (Nippgen et al., 2015; Saffarpour et al., 2016). As a result, R occurrence depends not only on P magnitude, but on the interaction between event characteristics and the dynamically evolving wetness state of the system, which together control the activation of hydrological coupling within the catchment (Bracken et al., 2013; Dymond et al., 2021; Garcia-Estringana et al., 2013; Latron and Gallart, 2008; Nanda and Safeeq, 2023).

In Mediterranean environments, this behaviour is further modulated by strong seasonality. Alternating wet, dry, and transitional periods, together with high evapotranspiration demand, generate pronounced temporal variability in SM that governs catchment responsiveness and the likelihood of hydrological coupling between landscape elements (Gallart et al., 2002; Garcia-Estringana et al., 2013; Latron and Gallart, 2007, 2008). During dry and drying-down conditions, low SM restricts the development of connected flow pathways and suppresses R, whereas wetter periods promote the activation and expansion of subsurface and lateral flow pathways, increasing the degree of hydrological coupling and enhancing the probability of outlet response (Detty and McGuire, 2010; Penna et al., 2011; Saffarpour et al., 2016).

At the event scale, previous studies highlighted the importance of both P characteristics (e.g., total depth and intensity) and SM conditions in controlling R generation (Assouline et al., 2024; Blume et al., 2009; Farrick and Branfireun, 2014; Gallart et al., 1994, 2002; Kaffas et al., 2025; Keller et al., 2023; Latron and Gallart, 2008; Nanda and Safeeq, 2023; Penna et al., 2011; Saffarpour et al., 2016; Scaife and Band, 2017). However, the role of different SM metrics remains unclear. While antecedent wetness has often been observed as a dominant control on R response (Llorens et al., 2018; Penna et al., 2011; Scaife and Band, 2017), metrics capturing intra-event scale dynamics—such as maximum SM and changes in SM (ΔSM)—may better reflect the processes governing the activation of hydrological coupling (Nanda and Safeeq, 2023; Singh et al., 2021), as they describe the transient filling of soil storage and the progression towards threshold conditions required for the initiation and connection of lateral flow pathways (McDonnell et al., 2021; Tromp-Van Meerveld and McDonnell, 2006).

https://doi.org/10.5194/egusphere-2026-2711
Preprint. Discussion started: 22 May 2026

Most of the previous studies have been focused on events that generate measurable R at the catchment outlet (Gallart et al., 2002; Keller et al., 2023; Latron and Gallart, 2008; Licciardello et al., 2019; Moreno-de-las-Heras et al., 2019; Nanda and Safeeq, 2023; Penna et al., 2011; Singh et al., 2021), potentially overlooking the hydrological relevance of non-flow events. However, non-flow events provide critical information on the conditions under which hydrological spatial coupling fails to develop (McDonnell et al., 2021), thereby helping constrain the thresholds and mechanisms of R generation. Ignoring these events may bias the identification of controlling factors and limit the interpretation of state-dependent hydrological responses. Despite their importance, relatively few studies have explicitly incorporated both flood and non-flow events in a unified analytical framework (e.g., Kaffas et al., 2025; Saffarpour et al., 2016). Addressing this limitation is essential for advancing a probabilistic understanding of R occurrence and identifying the conditions under which hydrological coupling is activated. This requires considering how water is spatially organized and transmitted within the catchment. The concept of hydrological connectivity provides a useful framework to describe how flow pathways are structured and activated across the landscape (Bracken et al., 2013; Turnbull and Wainwright, 2019; Wainwright et al., 2011). In this context, structural connectivity—defined by terrain attributes, soil properties, and anthropogenic features—controls the potential flow pathways, while functional connectivity reflects their dynamic activation under specific hydrological conditions (Turnbull et al., 2008; Wainwright et al., 2011). The extent to which local SM dynamics contribute to outlet R therefore depends on both landscape position and the degree to which these pathways become functionally connected. Building on this framework, R occurrence can be interpreted as the outcome of effective hydrological coupling across spatially distributed landscape elements, whereby local hydrological responses are propagated through the system and expressed as R at the outlet (Buttle et al., 2004; Calvo-Cases et al., 2021; Wainwright, 2006).

Terraced landscapes, which are widespread in Mediterranean regions, introduce additional complexity to hydrological processes. Stone walls and modified soil profiles alter both storage capacity and flow pathways, influencing the spatial organization of hydrological connectivity (Arnáez et al., 2015; Moreno-de-las-Heras et al., 2019; Preti et al., 2018). Terraces can act as both buffers and transmitters of R, depending on their structural connectivity and wetness conditions, leading to spatially variable and non-linear hydrological responses (Gallart et al., 1994). Despite their importance, the role of terraces in modulating event-scale R occurrence and its relation to SM dynamics is yet to be fully characterized, particularly in post-disturbance environments such as wildfires, which are recurrent and increasingly frequent in Mediterranean regions (Abatzoglou et al., 2019; Jones et al., 2022) and induce significant but time-dependent changes in vegetation cover, soil properties, and infiltration capacity (Certini, 2005; Shakesby, 2011). While their immediate hydrological impacts are often pronounced, these effects evolve over time as vegetation recovers and soil properties reorganize. As a result, post-fire hydrological responses reflect a combination of transient disturbance effects and longer-term ecohydrological recovery, which can continue to influence SM dynamics and flow pathways years after the event. However, the extent to which such legacy effects interact with structural features such as terraces and with seasonally varying SM conditions to control R occurrence demands further investigation.

https://doi.org/10.5194/egusphere-2026-2711
Preprint. Discussion started: 22 May 2026

Sa Font de la Vila River is a burned Mediterranean terraced catchment located in the island of Mallorca (Spain), where hydrological and sediment connectivity processes have been extensively investigated in recent years. Previous studies have examined post-fire hydrological response and sediment transport dynamics, highlighting the strong influence of terraces, vegetation recovery, and soil properties on R generation and connectivity patterns (e.g., Calsamiglia et al., 2017, 2018; Estrany et al., 2019a; García-Comendador et al., 2017; Lucas-Borja et al., 2018). These works have demonstrated how anthropogenic features such as terraces exert a key control on the spatial organization of connectivity, modulating both water and sediment fluxes across the catchment. However, despite this extensive body of research, the event-scale controls on R occurrence and their relationship with SM dynamics and hydrological coupling constitute a significant knowledge gap, particularly regarding how spatial connectivity translates into event-scale hydrological coupling and outlet R response.

This study addresses these gaps by investigating the controls on R occurrence and hydrological spatial coupling in one of the structurally complex terraced microcatchments of the Sa Font de la Vila River, affected by a high-severity wildfire. Using four years of high-resolution P, SM, and discharge (Q) data, all P events were systematically analyzed, regardless of whether they produced outlet R response. For each event, P and SM metrics were quantified to examine how seasonal conditions, event-scale SM dynamics, and spatial variability across hillslope and terrace positions interact to regulate R response. This approach enables the interpretation of R occurrence as a probabilistic response and provides insights into the state-dependent controls governing the activation of hydrological coupling in Mediterranean terraced catchments. Within this framework, the study (i) quantifies the seasonal variability of R occurrence and its relationship with SM dynamics; (ii) assesses the relative importance of P characteristics and different SM metrics (antecedent SM, maximum SM, and ΔSM) in controlling event-scale R occurrence; and (iii) evaluates how spatial variability in structural connectivity modulates the relationship between local SM dynamics and outlet response across the hillslope–terrace system. By integrating seasonal, event-scale, and spatial analyses, this study advances the understanding of the mechanisms governing hydrological coupling in Mediterranean terraced landscapes and highlights the importance of connectivity-based approaches for improving hydrological understanding and management under changing environmental conditions.

2 Materials and methods

2.1 Study area

The So na Vidala microcatchment (4.7 ha) is located at the headwaters of the representative Sa Font de la Vila River catchment, in the southwestern sector of the Tramuntana Range (Mallorca, Spain; Fig. 1a, b), recognised as a UNESCO World Heritage Cultural Landscape. It is a typical Mediterranean headwater system and was selected due to the coexistence of traditional soil and water conservation structures, and a well-documented history of forest transition and wildfire disturbance in the second half of the 20th century (Estrany et al., 2019).

https://doi.org/10.5194/egusphere-2026-2711
Preprint. Discussion started: 22 May 2026

Elevations range from 251 to 416 m a.s.l. (Fig. 1c), encompassing steep natural hillslopes and gently sloping abandoned agricultural terraces. Terraced landforms occupy 16.8 % of the microcatchment area and include three main types (Fig. 1d): (i) check-dam terraces (9.3 %), formed by small in-channel dry-stone check-dams where the natural creek is laterally diverted, promoting sediment retention and additional cultivable land while reducing channel erosion; (ii) field terraces (2.6%), characterized by relatively wide, gently sloping platforms constructed on moderate hillslopes for rainfed agriculture; and (iii) step terraces (4.9 %), consisting of narrow benches retained by dry-stone walls on steep slopes, designed to maximize arable land while controlling R and soil erosion. Although originally built for agriculture, terraces continue to shape the microcatchment, exerting a persistent ecogeomorphological and hydrological control on surface R, sediment redistribution, and SM patterns, despite variable preservation.

Lithology is dominated by Rhaetian dolomites and marls, which strongly influence soil development and hydrological behaviour. Soils on non-terraced hillslopes are generally shallow and weakly differentiated over carbonate bedrock, reflecting limited pedogenesis and commonly classified as Entisols (Soil Survey Staff, 1999). These soils exhibit poorly developed profiles, high stone content, and low water-holding capacity. Terraced areas, although still relatively shallow in absolute terms, are distinctly deeper than adjacent hillslopes and contain a higher fine-earth fraction, reflecting long-term sediment accumulation and historical anthropogenic soil management. Clear contrasts in soil quality emerge between hillslopes and terraces, with terraced soils having higher carbonate concentrations and alkalinity but lower organic matter, cation exchange capacity, and overall biological activity than non-terraced hillslope soils (Calsamiglia et al., 2017; Lucas-Borja et al., 2018).

Vegetation structure reflects the combined effects of post-abandonment succession and repeated wildfire disturbance (Fig. 1e, f), differing between hillslopes and terraces. Non-terraced hillslopes surrounding the monitored field terrace present lower vegetation cover, with discontinuous shrub and grass cover dominated by lentisk (*Pistacia lentiscus* L.), rosemary (*Salvia rosmarinus* Spenn.), *Anthyllis cytisoides* L., and *Erica multiflora* L. The herbaceous layer includes Mauritanian grass (*Ampelodesmos mauritanica* (Poir.) T. Durand & Schinz) and Mediterranean false brome (*Brachypodium retusum* (Pers.) P.Beauv.), the latter occurring mainly during periods of sufficient SM. Scattered small Aleppo pines (*Pinus halepensis* Mill.) are also present. In contrast, terraces support denser and more continuous vegetation, including larger Aleppo pines and scattered holm oak (*Quercus ilex* L.), together with a well-developed shrub layer dominated by lentisk, spiny broom (*Calicotome spinosa* (L.) Link), *Erica multiflora* L., and grey cistus (*Cistus albidus* L.), and a higher cover of Mediterranean false brome.

The climate is Mediterranean subhumid, with a mean annual temperature of 16.5 °C and average annual P of 491 mm (2013-2024; coefficient of variation: 25.7 %). Agricultural activities in the microcatchment were entirely abandoned in the 1960s, triggering widespread secondary succession and progressive afforestation. Since abandonment, the area has been affected by recurrent wildfires, further shaping its ecohydrological dynamics. Two major wildfires stand out: a partial burn in 1994 affecting the westernmost sector and a high-severity wildfire in 2013 that burned the entire microcatchment (Fig. 1e). Areas

https://doi.org/10.5194/egusphere-2026-2711
Preprint. Discussion started: 22 May 2026

affected by both wildfires are typically steep and show limited post-wildfire vegetation recovery, whereas areas burned only in 2013, particularly terraced zones, exhibit more advanced recovery, highlighting the long-term legacy of terracing on ecosystem resilience, as well as on ecohydrological responses.

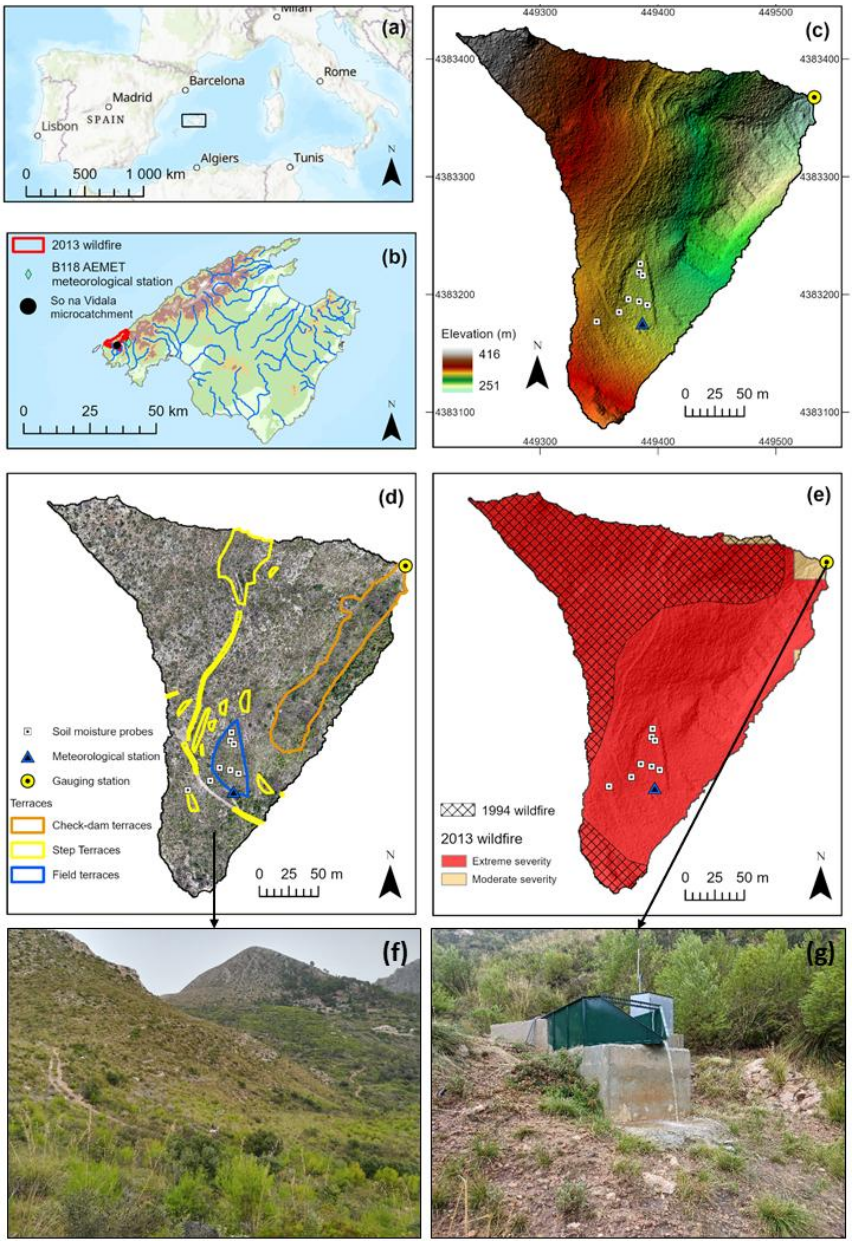

Figure 1: Location of the study area: (a) Mallorca within the Western Mediterranean Region; (b) the So na Vidala microcatchment, showing the extent of the area affected by the 2013 wildfire. The locations of the meteorological station, gauging station, and SM probes, together with the microcatchment boundaries, are shown along with: (c) a high-resolution digital elevation model (0.25 m px^{-1}); (d) the spatial distribution and typology of terraced areas derived from drone-based ortophotography; and (e) areas affected by the 1994 and 2013 wildfires, including 2013 burn severity estimated using the differenced Normalized Burn Ratio (dNBR). Views of (f) the microcatchment from the headwater area (southern sector) and (g) the H-flume installed at the microcatchment outlet.

https://doi.org/10.5194/egusphere-2026-2711
Preprint. Discussion started: 22 May 2026

2.2 Monitoring and data acquisition

In 2019, a programme of continuous environmental measurements was implemented at So na Vidala microcatchment. Meteorological variables were monitored at the headwaters. P was recorded with a tipping bucket rain gauge (Lambrecht 15189; Lambrecht meteo GmbH, Germany), air temperature and relative humidity using an HD 9009TRR sensor (Delta Ohm, Italy), wind speed and direction with a Wind Sentry 03002 (R.M. Young Company, USA), and a CNR-4 four component net radiation sensor (Kipp & Zonen, Netherlands).

Soil volumetric water content was monitored using Hydra Probe II sensors (Stevens Water Monitoring Systems, USA), which estimate SM from the complex dielectric permittivity of the soil. Sensors were installed within hillslope and terrace locations associated with a representative abandoned field terrace (Fig. 2a, b), in order to capture spatial variability in SM dynamics across the hillslope-terrace system. A total of 11 sensors were deployed at depths of 10 and 50 cm to characterize near-surface and subsurface SM conditions. Single sensors were installed vertically at 10 cm depth, whereas pairs of sensors were installed horizontally at 10 and 50 cm depth to capture vertical variability in SM profiles. The monitored locations included: (i) hillslope positions with contrasting slope gradients and high structural connectivity, represented by two vertically installed sensors at 10 cm depth (High-Connectivity Low-Gradient Hillslope and High-Connectivity High-Gradient Hillslope; Fig. 2d); (ii) terrace edge positions with high structural connectivity, represented by two vertically installed sensors at 10 cm depth near the upslope terrace edge (High-Connectivity Upslope-Edge Terrace 1, Fig. 2e; and High-Connectivity Upslope-Edge Terrace 2, Fig. 2c); (iii) a terrace interior position with low structural connectivity, represented by one vertically installed sensor at 10 cm depth (Low-Connectivity Mid-Terrace; Fig. 2e); (iv) a terrace interior position with very low structural connectivity, represented by two horizontally installed sensors at 10 and 50 cm depth (Disconnected Mid-Terrace; Fig. 2c); (v) a position adjacent to a well-preserved dry-stone wall, represented by two horizontally installed sensors at 10 and 50 cm depth (Intact Wall-Adjacent Terrace; Fig. 2c); and (vi) a position adjacent to a collapsed wall section, also represented by two horizontally installed sensors at 10 and 50 cm depth (Collapsed Wall-Adjacent Terrace; Fig. 2e).

These monitoring locations were selected to capture structural variability within the hillslope-terrace system and associated contrasts in structural hydrological connectivity. Structural connectivity conditions were assessed using the Sediment Connectivity Index (Crema and Cavalli, 2018; Estrany et al., 2019) derived from a high-resolution digital elevation model (0.25 m px^{-1}). Sensors were used with the manufacturer's factory calibration, without additional site-specific calibration, which is appropriate for identifying SM thresholds associated with R generation, as these thresholds are derived consistently across locations using the same sensor type and installation protocol.

All sensors were connected to a CR350 datalogger (Campbell Scientific, USA), which recorded data at 15-minute intervals, averaged from 1-minute readings. Daily reference evapotranspiration (ET_0) was estimated using the FAO-56 Penman-Monteith equation (Allen et al., 1998), based on the collected meteorological data.

https://doi.org/10.5194/egusphere-2026-2711
Preprint. Discussion started: 22 May 2026

Water stage was continuously recorded at the microcatchment outlet using an H-flume (Fig. 1g; OpenChannelFlow, USA). Stage measurements were initially obtained with a CS451-L pressure transducer (Campbell Scientific, USA; measurement range: 0-5.1 m), which was replaced in January 2023 by an OTT PLS sensor (OTT HydroMet, Germany; measurement range: 0-4 m). Recorded water stage was subsequently converted to Q using the manufacturer's rating curve specific to the H-flume geometry.

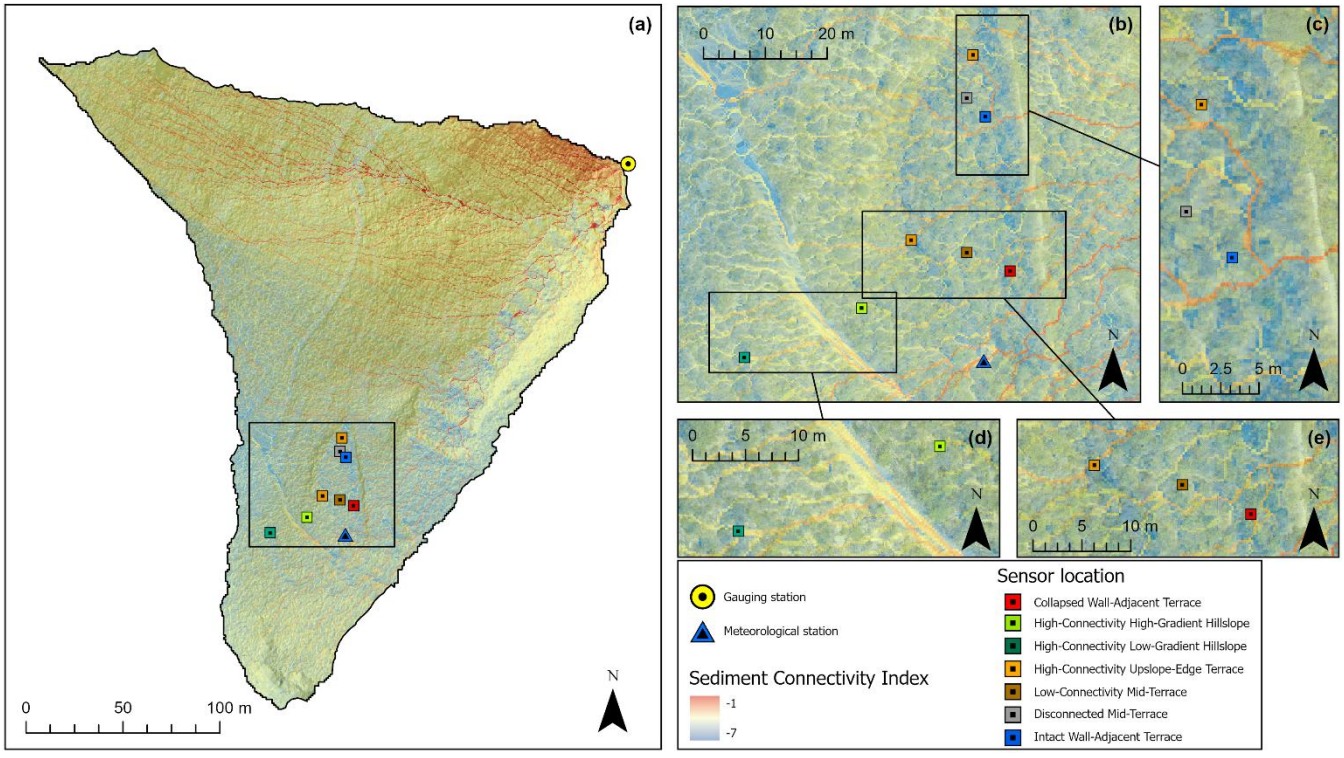

Figure 2: Sediment Connectivity Index (Crema and Cavalli, 2018) derived from a high-resolution digital elevation model (0.25 m px^{-1}), showing the location of SM probes in (a) So na Vidala microcatchment and (b) the surroundings of the monitored headwater field terrace, with zoom on (c) Disconnected Mid-Terrace, High-Connectivity Upslope-Edge Terrace 2, and Intact Wall-Adjacent Terrace locations; (d) High-Connectivity High-Gradient Hillslope and High-Connectivity Low-Gradient Hillslope locations; and (e) High-Connectivity Upslope-Edge Terrace 1, Low-Connectivity Mid-Terrace, and Collapsed Wall-Adjacent Terrace locations.

2.3 Rainfall – soil moisture – discharge seasonal assessment

P, SM, and Q dynamics were evaluated at both annual and seasonal scales using continuous monitoring data collected over a four-year period (2021-2024). Calendar years were used rather than hydrological years to ensure the inclusion of a larger number of events for analysis.

To capture intra-annual variability in rainfall-runoff dynamics, four hydrological seasons (wet, drying-down, dry, and wetting-up) were delineated following Garcia-Estringana et al. (2013). The classification was based on temporal patterns in SM, P, and ET_0. Wet seasons were defined as periods when SM remained consistently high, typically exceeding the 75th percentile of

https://doi.org/10.5194/egusphere-2026-2711
Preprint. Discussion started: 22 May 2026

the distribution calculated from the full monitoring period using the mean SM across all sensors. Dry seasons corresponded to periods when SM remained below the 25th percentile and P events produced only brief and limited increases in soil water content. Transitional periods -classified as wetting-up and drying-down- captured the progressive increase or decrease in SM, respectively, reflecting the reactivation or decline of functional hydrological connectivity within So na Vidala microcatchment.

2.4 Identification of events

To investigate the event-scale relationships between P, SM, and R generation, individual P events were identified. A P event was defined as any recorded P equal to or greater than 1 mm, which represented the minimum threshold capable of producing a measurable SM response exceeding the sensor accuracy (±1 %).

Events were further classified based on whether P produced measurable Q at the microcatchment outlet. A flood event was defined as one in which measurable Q occurred at the outlet within six hours following the onset of P. The end of a flood event was defined as the time when Q returned to zero, provided that no additional P occurred in the subsequent six hours. For non-flow events, the end of the P event was considered to occur after six consecutive hours without P (Nanda and Safeeq, 2023; Penna et al., 2011).

Given the absence of baseflow in the So na Vidala microcatchment, all R was attributed to stormflow processes. Applying these criteria, a total of 186 P events were identified over the study period (2021-2024), of which 31 produced measurable Q at the microcatchment outlet.

2.5 Statistical analysis of events metrics

For each P event, whether it generated flow at the outlet, storm duration, total P, and peak 15-min P intensity ($IP_{max}15$) were computed. SM metrics were also derived, including antecedent SM, average SM, maximum SM, and the event-scale SM change (ΔSM). Statistical differences between flood and non-flow events —both overall and within each season— were assessed using Shapiro-Wilk and Levene's tests to evaluate normality and variance homogeneity. Depending on these results, either t-tests or Mann–Whitney U tests were applied, with *p*-values corrected for multiple comparisons using the False Discovery Rate method. Analyses were conducted in R (version 4.3.2) using the *dplyr*, *car*, and *stats* packages, with significance set at an adjusted $p < 0.05$.

2.6 Soil moisture-discharge relationship analysis

To examine how SM conditions at different landscape positions relate to Q dynamics at the microcatchment outlet during flood events, SM-Q relationships were analyzed using 15-minute time series data. The analysis was restricted to timestamps during which Q was observed at the outlet. SM and Q were synchronized at matching timestamps, allowing characterization of the range, timing, and seasonal evolution of SM conditions locally associated with ongoing outlet Q.

https://doi.org/10.5194/egusphere-2026-2711
Preprint. Discussion started: 22 May 2026

3 Results

3.1 Rainfall, soil moisture and runoff dynamics

P, SM, and Q data collected between 2021 and 2024 (both included) were analyzed to evaluate hydrometeorological patterns in the microcatchment at different timescales, including the full study period, inter-annual variability, and seasonal dynamics.

3.1.1. Study period and inter-annual variation

At the annual scale, mean R depth over the study period was 1.79 mm, corresponding to a R coefficient of 0.37 % (Fig. 3a). Mean annual P was 496.9 ± 189.6 mm, showing strong inter-annual variability, whereas annual ET_0 remained relatively stable (1,199.9 ± 32.9 mm). Average SM during the study period was 20.4 ± 4.5 % at 10 cm depth and 23.5 ± 4.7 % at 50 cm depth, with slightly wetter conditions observed in 2021. A total of 186 P events were recorded, of which 31 (16.7 %) generated measurable R at the microcatchment outlet.

R was strongly concentrated in 2021, when total R reached 6.57 mm (91.5 % of total R during the study period), yielding the highest annual R coefficient (0.91 %; Fig. 3b-c). This was largely driven by an exceptionally wet November 2021, when 299.8 mm of P were recorded, contributing 72.9 % of total R. Comparison with the long-term P record from the nearby B118-AEMET station (4.5 km east of the microcatchment; Fig. 1b), operational since 1957, confirms that November 2021 was the wettest month on record in the area. In 2022, R depth was 0.02 mm (R coefficient = 0.006 %; Fig. 3d), while no measurable R was recorded in 2023 (Fig. 3e). A 45 mm P event on 27 August 2023 generated R, but data loss at the gauging station did not allow its quantification. In 2024, R increased slightly to 0.59 mm (8.2 % of total R), with a R coefficient of 0.1 % (Fig. 3f).

https://doi.org/10.5194/egusphere-2026-2711
Preprint. Discussion started: 22 May 2026

(a)

	Study period	2021	2022	2023	2024
Total rainfall (mm)	496.9 ± 189.6	725.8	313.6	372	562.2
Total reference evapotranspiration (mm)	1199.9 ± 32.9	1209.3	1226.3	1151.9	1212.2
Average soil moisture 10 cm (%)	20.4 ± 4.5	21.8	19.8	19.8	20.3
Average soil moisture 50 cm (%)	23.5 ± 4.7	25.2	23.2	22.1	23.4
Total runoff (mm)	1.79 ± 3.19	6.57	0.02	0	0.59
Runoff coefficient (%)	0.372	0.905	0.006	0	0.105

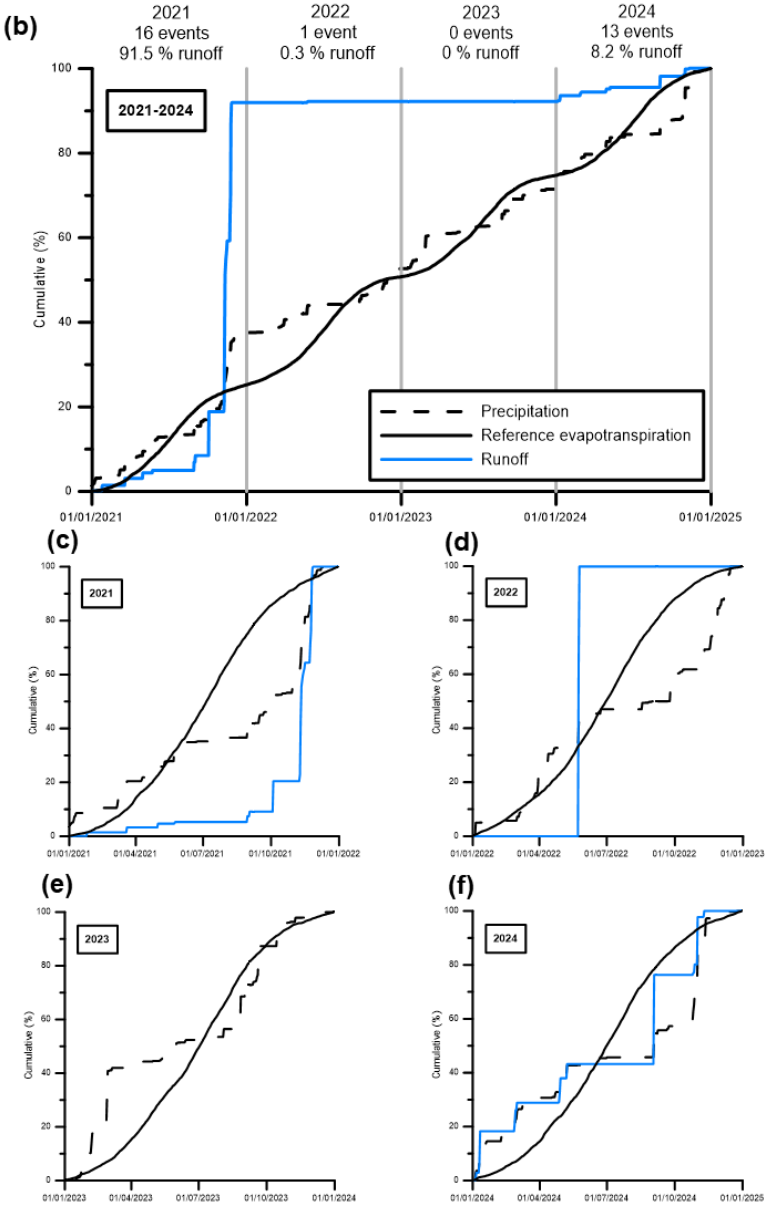

Figure 3: (a) Study period and inter-annual hydrometeorological conditions and runoff response during the study period (2021–2024). Values for the entire study period are presented as mean ± standard deviation, while mean annual values are shown for each year. Cumulative precipitation, reference evapotranspiration, and runoff for (b) the entire study period, (c) 2021, (d) 2022, (e) 2023, and (f) 2024.

https://doi.org/10.5194/egusphere-2026-2711
Preprint. Discussion started: 22 May 2026

3.1.2. Seasonal scale

ET_0 followed a pronounced seasonal cycle typical of Mediterranean conditions, with lowest values during late autumn and winter (1.76 ± 0.96 mm day^{-1} in wet periods) and progressively increasing during spring to peak in summer (4.26 ± 1.85 mm day^{-1} in dry periods) (Fig. 4). SM exhibited seasonal variation, with depletion during periods of higher ET_0 and recovery during periods of lower ET_0 and increased P inputs.

SM dynamics were strongly depth dependent. At 10 cm, SM responded rapidly to P and decreased sharply during periods of high atmospheric demand. At 50 cm, SM varied more gradually and within a narrower range, reflecting slower depletion and greater storage buffering.

Across the study period, five wet, drying-down, dry, and wetting-up seasons were identified (Fig. 4). Wet and dry seasons were the longest, while transitional seasons (i.e., drying-down and wetting-up) were shorter (Table 1). Wet periods accounted for 33.8 % of the study period, drying-down 20.3 %, dry 35.2 %, and wetting-up 10.7 %. The timing and duration of hydrological seasons varied between years depending on the interplay between P and ET_0. Transitions from wet to drying-down conditions occurred consistently during spring, when increasing ET_0 (up to ~4 mm day^{-1}) coincided with declining SM. However, seasonal progression was sensitive to P patterns. For example, in 2023, anomalously low autumn P limited SM recovery following summer depletion, resulting in two distinct dry periods separated by an incomplete wetting-up season.

Seasonal rainfall-runoff patterns corresponded to these hydrometeorological dynamics. Total P was highest during wet periods (178.8 ± 111.6 mm) and lowest during drying-down (42 ± 43.4 mm) and dry periods (48.6 ± 37.5 mm), while wetting-up seasons showed intermediate values (85.4 ± 71.9 mm) (Table 1). Daily ET_0 peaked during drying-down and dry seasons and was lowest during wet periods. R occurrence was strongly seasonal, with the highest total R and R coefficients during wet (4.1 mm; 0.42 %) and wetting-up seasons (2.65 mm; 0.54 %), and minimal R during drying-down (0.23 mm; 0.09 %) and dry seasons (0.2 mm; 0.08 %).

https://doi.org/10.5194/egusphere-2026-2711
Preprint. Discussion started: 22 May 2026

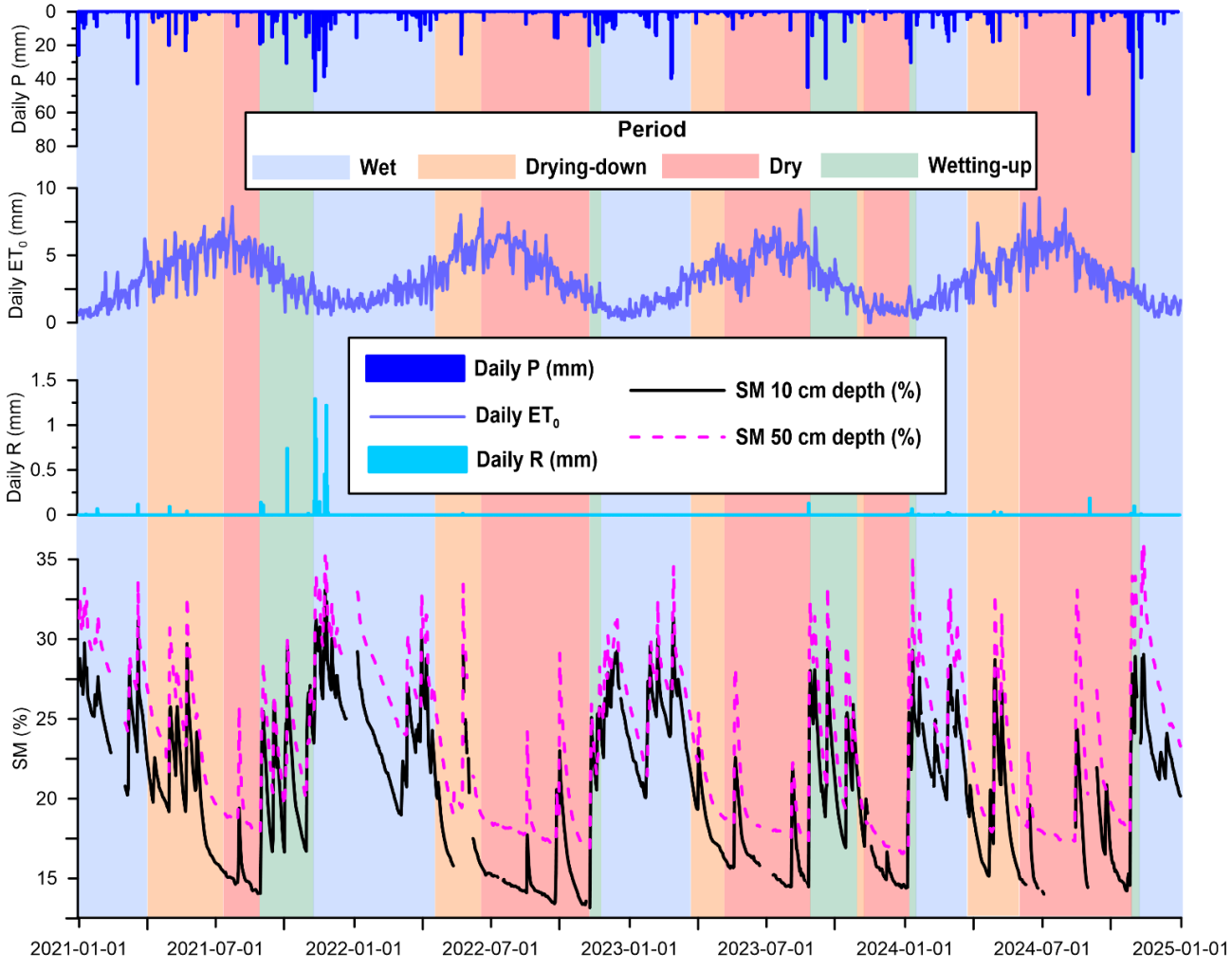

Figure 4: Daily hydrometeorological and soil moisture (SM) dynamics at So na Vidala microcatchment during the study period. Daily precipitation (P), reference evapotranspiration (ET_0), and runoff (R) are shown as daily totals. SM at 10 cm and 50 cm depths is presented as the daily mean across all sensors installed at each respective depth. Background colours indicate hydrological seasons: wet period (blue), drying-down period (orange), dry period (red), wetting-up period (green).

Table 1: Seasonal hydrometeorological conditions and runoff (R) response during the study period (2021–2024). Total precipitation (P) is reported as the mean ± standard deviation of seasonal totals across all seasons of each type. Daily reference evapotranspiration (ET_0) is reported as the mean ± standard deviation of daily values within each season type. Average soil moisture (SM) at 10 cm and 50 cm depth represents the mean of daily values across all days within each season type. Total R corresponds to the cumulative R summed across all seasons of each type. R coefficient is calculated as the ration between cumulative R and cumulative P across all seasons of the same type.

	Wet	Drying-down	Dry	Wetting-up
Duration (days)	99 ± 39	59 ± 33	103 ± 48	31 ± 32
Total P (mm)	178.8 ± 111.6	42 ± 43.4	48.6 ± 37.5	85.4 ± 71.9
Daily ET_0 (mm)	1.76 ± 0.96	4.15 ± 1.54	4.26 ± 1.85	2.99 ± 1.19

https://doi.org/10.5194/egusphere-2026-2711
Preprint. Discussion started: 22 May 2026

Average SM 10 cm (%)	24.8	19.6	15.8	22.2
Average SM 50 cm (%)	28.2	22.9	19.0	24.9
Total R (mm)	4.10	0.23	0.20	2.65
R coefficient (%)	0.42	0.09	0.08	0.54

3.2. Event-scale rainfall and soil moisture controls on runoff occurrence

To assess factors associated with event-scale R response, P characteristics (total P, storm duration, and $IP_{max}15$), and SM metrics (antecedent SM, average SM, maximum SM, and ΔSM) were compared between flood and non-flow events for the full study period and for each hydrological season (Table 2).

3.2.1. Study period dynamics

For the full study period, flood events showed significantly higher values for all P and SM metrics than non-flow events (Table 2; $p < 0.05$), with the largest differences observed for storm duration, total P, $IP_{max}15$, average SM, maximum SM, and ΔSM ($p < 0.001$). Only 7 % of P events with total P <10 mm ($n = 128$) generated outlet R, whereas 82 % of events with total P >30 mm ($n = 17$) produced measurable outlet Q. Despite significant differences in mean values (Table 2; $p < 0.05$), flood and non-flow events overlapped in antecedent SM at both depths (Fig. 5a-b), indicating that initial wetness conditions do not determine outlet R occurrence. In contrast, average SM (Fig. 5c-d), maximum SM (Fig. 5e-f), and ΔSM (Fig. 5g-h) showed greater separation between event types, suggesting that progressive soil wetting during events and the attainment of high SM conditions are key controls on the activation of hydrological coupling and flow transmission to the outlet.

Table 2: Event-scale comparison of P and SM variables between flood and non-flow P events for the entire study period and for each hydrological season. Values are presented as mean ± standard deviation. SM metrics at 10 and 50 cm depth are calculated for each sensor and then averaged across all sensors installed at the corresponding depth. Event counts (*n*) indicate the total number of P events within each season. Statistical significance refers to differences between flood and non-flow events and is indicated as follows: ***$p < 0.001$, **$p < 0.01$, *$p < 0.05$. "Not significant" indicates $p \geq 0.05$. "-" indicates that the statistical test could not be performed due to the presence of only one quantified flood event during the dry season.

Metric	Season	Flood events	Non-flow events	Significance
Storm duration (h)	**Study period ($n = 186$)**	**13.4 ± 13.5**	**6.3 ± 8.6**	***
	Wet ($n = 81$)	13.4 ± 9.5	8.2 ± 7.4	*
	Drying ($n = 28$)	17.4 ± 20.9	4.7 ± 4.6	Not significant
	Dry ($n = 34$)	1.0	3.2 ± 2.9	-
	Wetting ($n = 43$)	16.4 ± 19.1	7.0 ± 13.9	Not significant
Total P (mm)	**Study period**	**25.6 ± 20.4**	**6.5 ± 8.7**	***
	Wet	23.8 ± 20.1	8.1 ± 11.2	***
	Drying	30.1 ± 10.5	3.7 ± 3.1	***
	Dry	49.0	4.6 ± 3.8	-
	Wetting	35.2 ± 25.4	6.5 ± 5.5	**
	Study period	**24.6 ± 27.1**	**7.3 ± 9.2**	***

https://doi.org/10.5194/egusphere-2026-2711
Preprint. Discussion started: 22 May 2026

$IP_{max}15$ (mm h^{-1})	Wet	17.3 ± 18.3	5.8 ± 4.8	***
	Drying	32.6 ± 36.4	3.3 ± 2.4	**
	Dry	119.2	9.4 ± 11.0	-
	Wetting	35.8 ± 19.8	9.4 ± 12.2	**
Antecedent SM 10 cm (%)	**Study period**	**23.5 ± 4.3**	**21.3 ± 4.5**	*
	Wet	26.5 ± 1.9	24.4 ± 3.4	*
	Drying	18.3 ± 1.7	19.7 ± 2.1	Not significant
	Dry	-	15.7 ± 1.4	-
	Wetting	20.6 ± 3.8	21.7 ± 4.3	Not significant
Antecedent SM 50 cm (%)	**Study period**	**26.3 ± 5.1**	**23.9 ± 4.4**	*
	Wet	30.1 ± 2.1	27.3 ± 3.1	***
	Drying	21.4 ± 2.8	22.9 ± 2.8	Not significant
	Dry	-	18.5 ± 1.2	-
	Wetting	22.1 ± 4.4	23.1 ± 3.7	Not significant
Average SM 10 cm (%)	**Study period**	**29.1 ± 2.4**	**22.8 ± 4.7**	***
	Wet	30.3 ± 2.0	26.0 ± 3.4	***
	Drying	27.1 ± 2.2	20.0 ± 2.1	***
	Dry	-	17.1 ± 2.3	-
	Wetting	27.9 ± 2.1	23.6 ± 3.7	**
Average SM 50 cm (%)	**Study period**	**31.9 ± 3.2**	**24.8 ± 4.8**	***
	Wet	33.3 ± 2.4	28.3 ± 3.6	***
	Drying	29.9 ± 3.3	22.9 ± 2.9	***
	Dry	-	19.6 ± 2.7	-
	Wetting	30.5 ± 3.3	24.3 ± 4.1	***
Maximum SM 10 cm (%)	**Study period**	**36.8 ± 3.7**	**25.1 ± 6.1**	***
	Wet	37.3 ± 3.8	28.6 ± 5.1	***
	Drying	36.2 ± 3.2	21.5 ± 3.4	***
	Dry	-	18.8 ± 4.1	-
	Wetting	36.1 ± 4.1	26.2 ± 5.0	***
Maximum SM 50 cm (%)	**Study period**	**37.9 ± 3.5**	**26.2 ± 6.0**	***
	Wet	37.8 ± 3.0	29.9 ± 5.0	***
	Drying	38.6 ± 3.2	23.2 ± 3.1	***
	Dry	-	21.1 ± 5.3	-
	Wetting	37.6 ± 4.7	25.8 ± 5.2	***
Δ SM 10 cm (%)	**Study period**	**13.0 ± 4.9**	**3.8 ± 4.4**	***
	Wet	10.8 ± 4.3	4.4 ± 4.1	***
	Drying	17.4 ± 5.0	1.9 ± 3.0	***

https://doi.org/10.5194/egusphere-2026-2711
Preprint. Discussion started: 22 May 2026

	Dry	-	2.8 ± 4.1	-
	Wetting	14.9 ± 3.7	4.9 ± 5.5	***
Δ SM 50 cm (%)	**Study period**	**11.5 ± 5.7**	**2.2 ± 4.1**	***
	Wet	8.0 ± 3.7	2.6 ± 3.9	***
	Drying	16.2 ± 5.3	0.4 ± 0.8	***
	Dry	-	2.2 ± 4.9	-
	Wetting	15.7 ± 4.7	2.8 ± 4.7	***

https://doi.org/10.5194/egusphere-2026-2711
Preprint. Discussion started: 22 May 2026

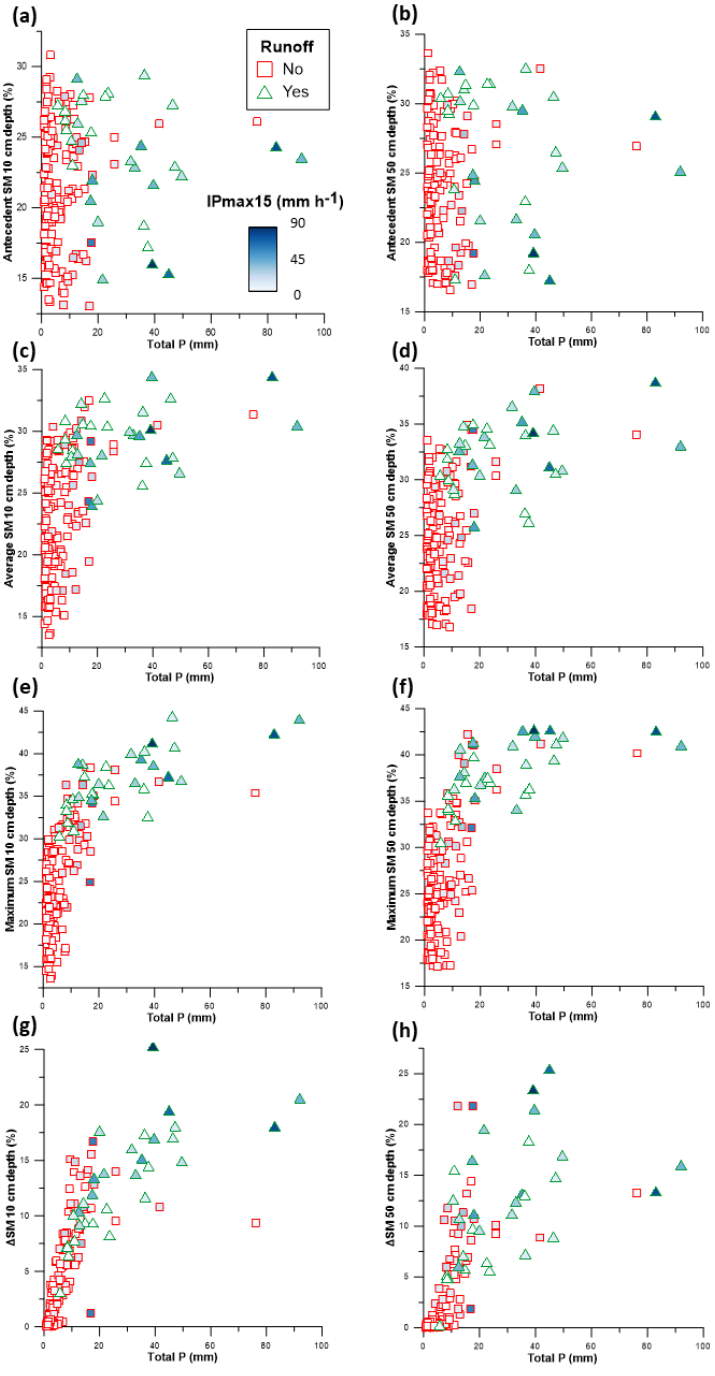

Figure 5: Event-scale relationships between flood and non-flow events for the full study period between total P and antecedent SM at (a) 10 cm and (b) 50 cm depth, average SM at (c) 10 cm and (d) 50 cm depth, maximum SM at (e) 10 cm and (f) 50 cm depth, and ΔSM at (g) 10 cm and (h) 50 cm depth. SM metrics values at each depth represent the mean across all sensors installed at that depth. Symbols represent individual P events. Flood events are indicated by green-outlined triangles and non-flow events by red-outlined squares. Symbol colour represents $IP_{max}15$ for each P event.

https://doi.org/10.5194/egusphere-2026-2711
Preprint. Discussion started: 22 May 2026

3.2.2. Seasonal patterns

Seasonal comparisons indicated that differences between flood and non-flow events varied among P characteristics and SM metrics (Table 2; $p < 0.05$). Total P and $IP_{max}15$ were significantly higher for flood events during wet ($p < 0.001$), drying-down ($p < 0.01$), and wetting-up ($p < 0.01$) seasons. Average SM, maximum SM, and ΔSM were also significantly higher during flood events across all seasons where statistical comparison was possible ($p < 0.01$).

In contrast, antecedent SM differed significantly between flood and non-flow events only during the wet season ($p < 0.05$), while no significant differences were observed during drying-down or wetting-up periods ($p \geq 0.05$). Storm duration exhibited a similar pattern, being significantly longer for flood events only during the wet season ($p < 0.05$).

Only two flood events were recorded during the dry season, not allowing statistical comparison. However, both were associated with high-magnitude P events, including the highest $IP_{max}15$ observed during the study period (119.2 mm h^{-1}).

3.3 Spatial variability in soil moisture controls on runoff response

Based on their consistent discrimination between event types across seasons, maximum SM and ΔSM were selected to further examine how spatial variability in SM dynamics and structural connectivity influenced outlet R response across the hillslope-terrace system.

3.3.1. Rainfall dynamics and soil moisture spatial patterns controlling runoff

Relationships between total P, maximum SM, ΔSM, and $IP_{max}15$ were analysed for a subset of representative monitoring locations across the hillslope-terrace system. From the full sensor network ($n = 11$), three probes (all at 10 cm depth) were selected to represent contrasting structural connectivity conditions: a high-connectivity low-gradient hillslope, a high-connectivity upslope-edge terrace, and a disconnected mid-terrace (Figs. 2, 6, 7). These locations capture the range of SM responses observed across the network, also noting that similar patterns were observed at both depths (Supplementary Tables 1-3).

At the high-connectivity low-gradient hillslope, both maximum SM and ΔSM showed clear seasonal patterns in relation to R occurrence (Figs. 6a-c, 7a). During the wet season, flood events were generally associated with higher maximum SM (Fig. 6a), while ΔSM overlapped substantially between event types, indicating limited event-scale increases under already wet conditions. In contrast, during the drying-down season, flood events coincided with both higher maximum SM and larger ΔSM, showing clearer separation from non-flow events. During the wetting-up period, maximum SM provided stronger discrimination than ΔSM, suggesting that R occurrence was more closely linked to saturation processes during events. Several wet-season flood events occurred under relatively low total P, coinciding with periods of high antecedent wetness (e.g.,

https://doi.org/10.5194/egusphere-2026-2711
Preprint. Discussion started: 22 May 2026

November 2021), when elevated antecedent SM promoted widespread functional connectivity across the hillslope-terrace system. Overall, R occurrence was consistently associated with high SM conditions at hillslope locations, being ΔSM more relevant during the drying-down season. Flood events were only observed when maximum SM exceeded approximately 32.5 %, although similar values also occurred during non-flow events (Fig. 6a-c).

At the high-connectivity upslope edge-terrace, maximum SM remained relatively high across seasons (Fig. 6d-f), likely reflecting enhanced water retention and lateral redistribution at the terrace edge. As a result, both maximum SM and ΔSM showed substantial overlap between flood and non-flow events (Fig. 7b). Limited separation between event types was observed during the wet and wetting-up periods (Fig. 6d, f), with only slightly greater differentiation during the drying-down season (Fig. 6e), when lower antecedent SM conditions increased the discriminative capacity of event-scale soil wetting. In contrast, total P showed a clearer association with R occurrence, particularly during transitional seasons, although overlap between event types persisted during the wet season. These patterns suggest that, at this highly connected terrace location, SM metrics alone did not clearly distinguish between event types, and outlet R occurrence was more closely related to P magnitude. Nevertheless, flood events were generally associated with maximum SM values above ~42.5 % during wet and wetting-up periods and ~45 % during the drying-down period, despite substantial overlap with non-flow events (Fig. 6d-e).

At the disconnected mid-terrace, maximum SM values were consistently lower than at the other locations and showed minimal separation between flood and non-flow events, except for slight differentiation during the drying-down season (Fig. 6g-i). ΔSM exhibited stronger seasonal variability. During the wet season, values overlapped substantially between event types, whereas during drying-down and wetting-up periods, flood events were more frequently associated with larger ΔSM, although overlap remained (Fig. 7c). Total P provided the clearest separation between event types during these transitional periods. These results indicate a weak relationship between local SM dynamics and outlet R occurrence at this disconnected location, with larger P inputs required to overcome local storage deficits and promote hydrological coupling with the rest of the microcatchment. Flood events were only observed above maximum SM values of approximately 16 % during wet periods, 17.5 % during drying-down, and 13 % during wetting-up periods, although these conditions were not exclusive to flood events (Fig. 6g-i).

https://doi.org/10.5194/egusphere-2026-2711
Preprint. Discussion started: 22 May 2026

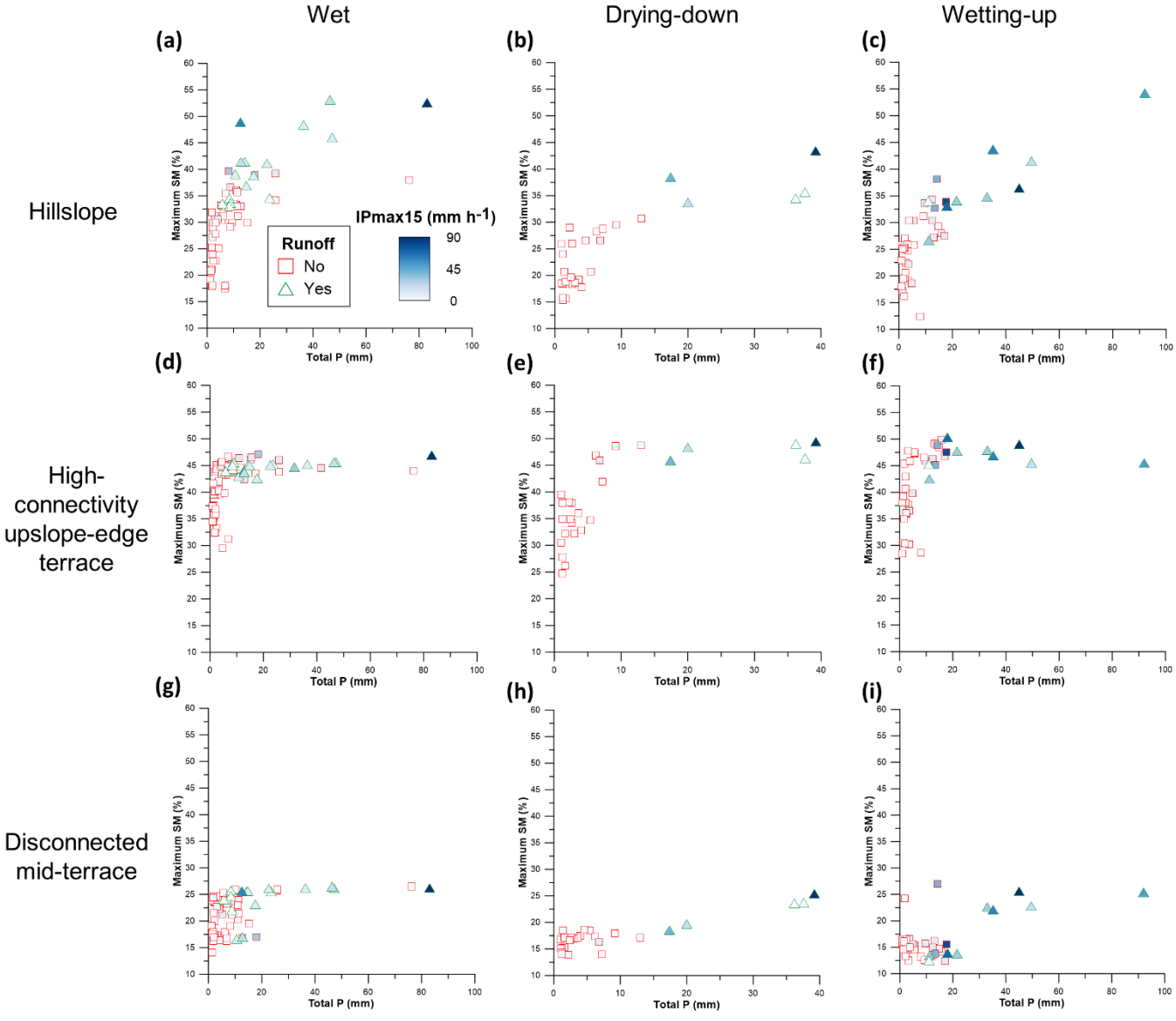

385 **Figure 6: Event-scale relationships between flood and non-flow events between total P and maximum SM for low-gradient high-connectivity hillslope during (a) wet, (b) drying-down, and (c) wetting-up seasons; for high-connectivity upslope-edge terrace 1 during (d) wet, (e) drying-down, and (f) wetting-up seasons; and for the disconnected mid-terrace during (g) wet, (h) drying-down, and (i) wetting-up seasons. Symbols represent individual P events. Flood events are indicated by green-outlined triangles and non-flow events by red-outlined squares. Symbol colour represents $IP_{max}15$ for each P event.**

390

https://doi.org/10.5194/egusphere-2026-2711
Preprint. Discussion started: 22 May 2026

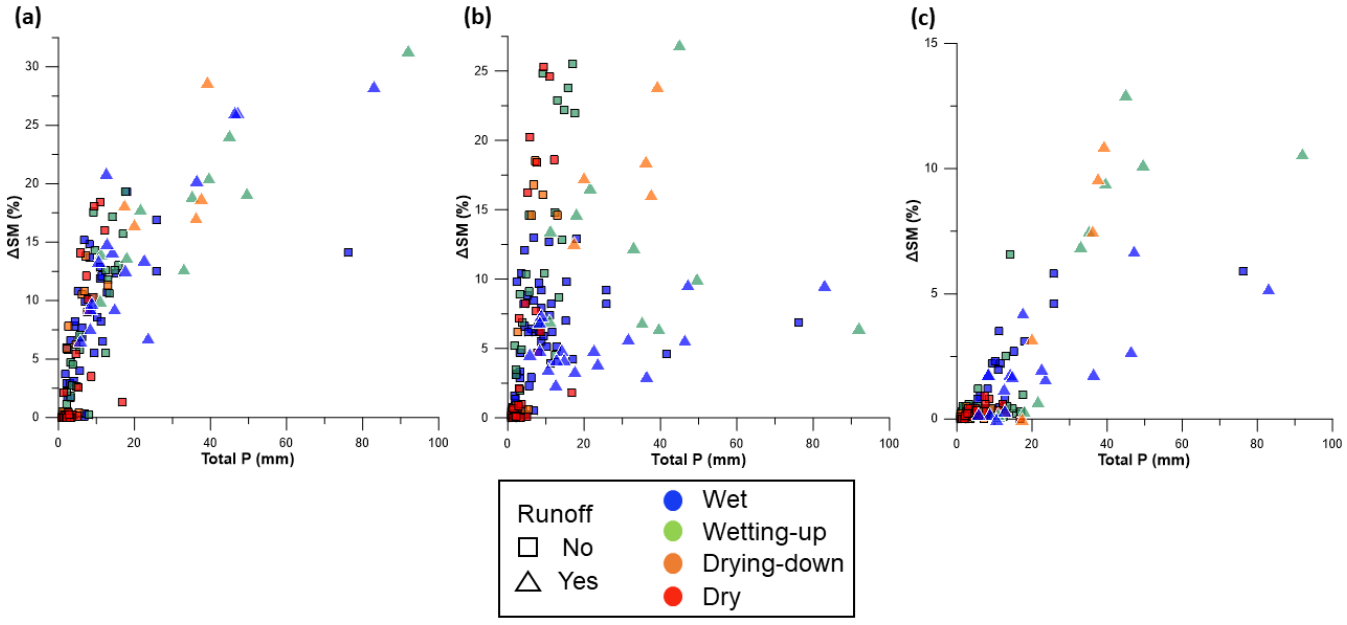

Figure 7: Event-scale relationships between flood and non-flow events for each hydrological season between total P and ΔSM for (a) low-gradient high-connectivity hillslope, (b) high-connectivity upslope-edge terrace 1, and (c) disconnected mid-terrace. Symbols represent individual P events. Flood events are indicated by triangles and non-flow events by squares. Symbol colours represent hydrological seasons.

3.3.2 Soil moisture conditions at representative locations and discharge at the microcatchment outlet

To further examine the relationship between local SM conditions and outlet R occurrence at the microcatchment outlet, SM-Q relationships were analyzed for the same three representative locations introduced in Sect. 3.2.2 (Fig. 8). Unlike the event-scale analysis from Sect. 3.2, this approach was restricted to time steps with observed outlet Q, examining instantaneous relationships between local SM and outlet Q.

At the high-connectivity low-gradient hillslope, outlet Q was associated with a broad range of local SM values, indicating weakly constrained coupling between local wetness conditions and outlet response (Fig. 8a). R occurrence coincided with lower SM values than those observed at the high-connectivity upslope-edge terrace 1, particularly during the drying-down season, when some high-intensity P events were associated with outlet Q under drier local conditions. This pattern was not observed during the wetting-up period, when Q occurred under higher SM conditions. A lower bound of SM associated with outlet Q was nevertheless identifiable, indicating that Q was not observed below a minimum range of local wetness conditions. As in Sect. 3.2.2, this behaviour was consistent across hillslope locations monitored in the hillslope-terrace system.

At the high-connectivity upslope-edge terrace 1, outlet Q was consistently associated with high SM values across all seasons (Fig. 8b). The range of SM conditions corresponding to Q occurrence remained similar between wet and transitional periods,

https://doi.org/10.5194/egusphere-2026-2711
Preprint. Discussion started: 22 May 2026

with substantial overlap and, in some cases, higher SM values during transitional seasons. Compared to hillslopes, SM values associated with Q were both higher and less variable, indicating a closer correspondence between local SM conditions and outlet Q response at this location. Variability in Q magnitude within similar SM ranges further reinforce that P characteristics also influence the R response.

At the disconnected mid-terrace, outlet Q was associated with lower SM than at the other locations and showed high variability, particularly across seasons (Fig. 8c). During transitional periods, outlet Q frequently occurred without within-event marked changes in local SM, indicating that R response was not directly reflected in local SM dynamics at this position. In contrast, during the wet season, Q occurrence was confined to a narrower range of higher SM values under sustained wet conditions. This pattern indicates limited correspondence between local SM dynamics and outlet R response at this location.

Across the three locations, SM-Q relationships reveal contrasting degrees of hydrological coupling associated with structural connectivity. The hillslope exhibited a wide range of SM conditions associated with Q occurrence, the upslope-edge terrace showed a more constrained and consistently high SM range, and the disconnected mid-terraced displayed weak and variable correspondence with outlet R response. Seasonal conditions further influenced these relationships. During wet periods, SM conditions associated with Q were more consistent across locations, whereas during drying-down and wetting-up periods, the range of SM associated with Q increased, particularly at the hillslope and disconnected mid-terrace, indicating greater variability in the conditions under which outlet R response occurred.

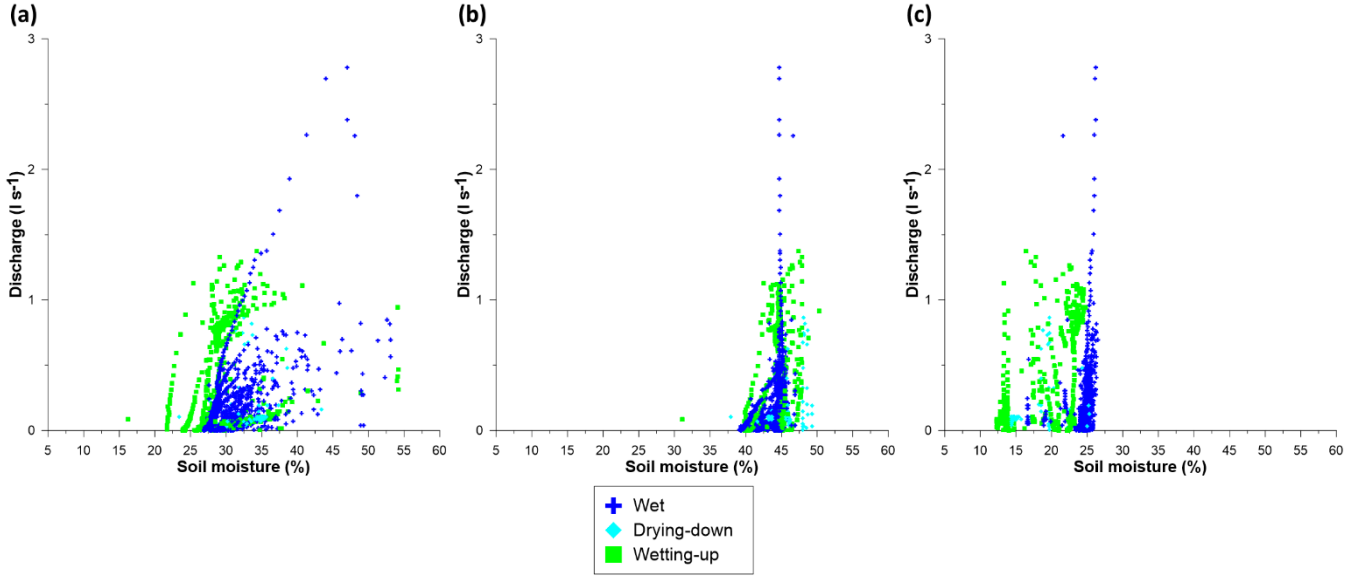

Figure 8: Timestamp-scale relationships between SM and Q at the microcatchment outlet across SM monitoring locations: (a) high-connectivity low-gradient hillslope, (b) high-connectivity upslope-edge terrace 1, and (c) disconnected mid-terrace at 10 cm depth.

https://doi.org/10.5194/egusphere-2026-2711
Preprint. Discussion started: 22 May 2026

4 Discussion

4.1 Process-based controls on hydrological coupling and runoff occurrence at different time scales

R response in the So na Vidala microcatchment was highly episodic, with only a small fraction (i.e., 16.7 %) of P events producing measurable outlet Q. This pattern reflects the dominant influence of infiltration, retention, and subsurface redistribution processes typical of Mediterranean terraced systems (Fortesa et al., 2020; Gallart et al., 1994; Moreno-de-las-Heras et al., 2019), where internal storage imposes strong constraints on flow generation. The resulting extremely low R coefficients further indicate that effective hillslope-channel coupling is only activated under specific combinations of P inputs and SM conditions (Bracken et al., 2013; Gallart et al., 1994; Latron and Gallart, 2008; McDonnell et al., 2021), rather than as a simple linear response to either factor alone.

4.1.1 Annual and seasonal scales

R occurrence was strongly seasonal, with most flood events concentrated during wet and wetting-up periods, while drying-down and dry seasons produced minimal R. This seasonal asymmetry reflects how the system's internal state, shaped by SM, P, and atmospheric demand, controls the likelihood of outlet response. A few high-magnitude storms, most notably during the anomalously wet November 2021, contributed disproportionately to total R, illustrating the non-linear behavior of Mediterranean hydrological systems, where extreme events dominate annual water yield (García-Comendador et al., 2017; Licciardello et al., 2019). Under climate change, Mediterranean catchments are also likely to experience more pronounced drought-flood abrupt alternation -DFAA, as longer dry spells and more intense rainfall increase the probability of rapid transitions from drought to flood across the region (Xiong and Yang, 2024).

SM dynamics emerged as a central control on R occurrence, influencing both the timing and persistence of hydrological coupling across microcatchment compartments. Shallow soil layers responded rapidly to P inputs, whereas deeper layers acted as gradual reservoirs, sustaining lateral flow and prolonging functional connectivity across the microcatchment. Under dry, drying-down, and early wetting-up conditions, limited SM reduced hydrological coupling between microcatchment compartments, requiring larger P inputs to activate downslope flow transmission. In these conditions, outlet R occurrence primarily reflected the activation of hillslope flow paths, while terraces likely functioned as transient SM sinks, temporarily storing water and attenuating downslope transmission (Garcia-Estringana et al., 2013; Moreno-de-las-Heras et al., 2019). By contrast, during wet and late wetting-up periods, elevated SM promoted more sustained hydrological coupling, enabling even low-magnitude P events to overcome minimal storage deficits and trigger an integrated response at the microcatchment outlet (Garcia-Estringana et al., 2013; Penna et al., 2011; Saffarpour et al., 2016).

https://doi.org/10.5194/egusphere-2026-2711
Preprint. Discussion started: 22 May 2026

These seasonal transitions were further shaped by hydrological memory. Successive P events during wetting-up periods progressively increased SM under lower ET_0 conditions, promoting the activation of functional connectivity and leading to wet conditions. In contrast, during drying-down seasons, increasing ET_0 and plant water use during spring supported progressive decoupling within the microcatchment. Occasional storms could temporarily increase SM and re-establish hydrological coupling, activating outlet R occurrence, although this connectivity was less persistent than during wetting-up and wet periods due to higher atmospheric demand. As a result, similar P inputs could lead to contrasting hydrological responses depending on whether the system was transitioning towards wetter or drier conditions (Latron et al., 2008; Nanda and Safeeq, 2023).

Overall, R occurrence reflects the seasonal reorganization of hydrological connectivity within the microcatchment, driven by the interplay between P inputs, SM dynamics, atmospheric demand, and landscape structure. Structural connectivity defines the potential flow pathways across the system (Bracken et al., 2013; Wainwright et al., 2011), but R generation depends on their temporal activation, such that hydrological coupling is only established when SM conditions allow effective flow transmission between landscape elements (McDonnell et al., 2021; Penna et al., 2011). As a result, the system alternated between phases of limited and effective coupling, rather than responding directly to P magnitude alone. During periods of higher SM, enhanced coupling promoted efficient propagation of subsurface flow towards the outlet, whereas under drier conditions, coupling remains weak or transient, limiting flow transmission despite the occurrence of P events (Nippgen et al., 2015; Saffarpour et al., 2016). In terraced landscapes, this behavior was further modulated by anthropogenic structures that alter the spatial organization and activation of flow pathways (Calsamiglia et al., 2018; Moreno-de-las-Heras et al., 2019; Preti et al., 2018), influencing the degree to which hillslope and terrace units become hydrologically coupled. Ultimately, R generation by the dynamic activation of connectivity, whereby the degree and persistence of hydrological coupling determined whether local hydrological responses were converged and delivered at the outlet (Masselink et al., 2017; Turnbull and Wainwright, 2019).

4.1.2 Event-scale controls on runoff occurrence

At the event scale, outlet R occurrence was controlled by the combined influence of P characteristics and SM dynamics. Flood events consistently occurred under higher total P and IP_{max15}, as well as higher average SM, maximum SM, and ΔSM compared to non-flow events (Table 2; Fig. 5). However, the overlap in antecedent SM indicates that initial wetness alone did not determine whether R occurred. Instead, R occurrence reflected the interaction between P inputs and the evolution of SM during events (Assouline et al., 2024; Scaife and Band, 2017), which governs the activation of hydrological coupling.

Seasonal variations modulated the interactions between P and SM characteristics unevenly. Total P and $IP_{max}15$ remained consistently associated with R occurrence across seasons, confirming their role as primary triggers. Similarly, maximum SM and ΔSM systematically distinguished between flood and non-flow events, indicating that both the peak wetness reached

https://doi.org/10.5194/egusphere-2026-2711
Preprint. Discussion started: 22 May 2026

during events and the magnitude of event-scale soil wetting are key controls throughout the year. In contrast, antecedent SM showed significant discrimination only during the wet season, when soils approached saturation and relatively small P inputs could trigger outlet Q (Fortesa et al., 2020). During drying-down and wetting-up periods, its predictive capacity diminished, reflecting reduced spatial hydrological coupling across the microcatchment and a stronger dependence on P magnitude to overcome SM deficits and trigger R occurrence.

Rather than acting independently, SM metrics captured complementary aspects of the system's hydrological behaviour, with their relative importance varying with season, soil conditions, and landscape position (Dymond et al., 2021; Singh et al., 2021). Maximum SM emerged as a robust indicator of R occurrence, particularly during transitional periods. Flood events were associated with the attainment of high SM conditions, suggesting the interpretation that R generation depends on reaching critical SM conditions required for lateral flow activation, consistent with the concept of dynamic storage thresholds in catchments (Nanda and Safeeq, 2023; Scaife and Band, 2017).

ΔSM provided additional insight into the mechanisms underlying this behaviour. The association between large ΔSM and R occurrence during drying-down and wetting-up periods is consistent with a fill-and-spill mechanism, in which subsurface storage must be progressively replenished before lateral flow pathways become connected (McDonnell et al., 2021). Under this framework, ΔSM reflects the transient filling of storage compartments required to re-establish hydrological coupling to the outlet. Similar behaviour was observed in small headwater catchments in California's Sierra Nevada, where deep soil wetting is necessary to activate lateral flow (Nanda and Safeeq, 2023). During wet periods, however, ΔSM became less informative, as near-saturated conditions limit further SM increases even during flood events.

On the other hand, antecedent SM showed limited predictive power overall, consistent with findings in semiarid Arizona (Zhang et al., 2011), but contrasting with studies where antecedent wetness was a dominant control (Llorens et al., 2018; Penna et al., 2011; Scaife and Band, 2017). This may reflect drier baseline conditions in So na Vidala or methodological differences, as this study assessed the ability of antecedent SM to predict whether outlet Q would occur or not, rather than describing its role only for flood events. In this study, its relevance was restricted to wet conditions, when soil was closed to saturation and even modest P inputs could trigger outlet Q, once a context-dependent threshold was exceeded (Fortesa et al., 2020). During transitional periods, its reduced predictive capacity likely reflected vertical redistribution processes and limited hydrological connectivity between microcatchment compartments, which decoupled shallow SM conditions from broader hydrological response (Grayson et al., 1997; Saffarpour et al., 2016).

4.1.3 Spatial variability in event-scale runoff controls across landscape positions

Spatial variability across the hillslope-terrace system added an additional layer of complexity to event-scale R controls (Merz and Plate, 1997), as the relationship between local SM dynamics and outlet R occurrence varied according to structural

https://doi.org/10.5194/egusphere-2026-2711
Preprint. Discussion started: 22 May 2026

connectivity. At high-connectivity hillslope locations, R occurrence closely tracked both maximum SM and ΔSM, indicating stronger coupling between local SM dynamics and outlet response. In contrast, terrace positions exhibited weaker and more variable relationships. At the high-connectivity upslope-edge terrace, R occurrence was more strongly associated with P magnitude than with local SM conditions, suggesting partial decoupling between local storage dynamics and microcatchment-scale response. This likely reflects the limited discriminative capacity of SM controls at this location, where relatively high maximum SM and ΔSM values are also observed during non-flow events due to its near-flat topographic position and high structural connectivity. This decoupling, although arising from different underlying mechanisms, was even more pronounced at the disconnected mid-terrace, where outlet R occurrence depended primarily on large P inputs capable of overcoming local storage deficits, reflecting structural disconnection that limits the transmission of local SM dynamics to the outlet.

These spatial contrasts in the relationship between SM dynamics and outlet R occurrence therefore suggest that the hydrological relevance of local wetness conditions depends on landscape position and structural connectivity (Dymond et al., 2021; Singh et al., 2021). While hillslope locations showed clearer association between SM dynamics and outlet response, terrace positions exhibited weaker or more variable relationships, particularly under disconnected conditions. These patterns are consistent with previous observations that R generation in Mediterranean catchments depends on the development of sufficiently wet conditions during events (Fortesa et al., 2020), while terraces exert strong spatial controls on the activation and transmission of hydrological connectivity (Calsamiglia et al., 2018).

4.2 Spatial organization of soil moisture-discharge: functional connectivity across landscape positions

Building on the event-scale controls described above, spatial variability in SM-Q relationships provides further insight into how functional hydrological connectivity is structured across the hillslope-terrace system. Local SM dynamics were not uniformly reflected in outlet Q, and the degree of correspondence varied substantially between landscape positions. While these patterns did not provide direct evidence of flow pathways, they allowed inference of where and when local wetness is more closely linked to the integrated microcatchment response.

4.2.1 Hillslopes

At hillslope locations, outlet Q occurred across a wide range of local SM conditions, including relatively dry states during drying-down periods. This broad range reflects weakly constrained coupling between local SM and outlet response, indicating that local wetness at these positions is only partially associated with outlet Q. Such behaviour is consistent with conditions in which P inputs can trigger outlet Q even under relatively low SM, particularly during high-intensity events (Nanda et al., 2019; Srinivasan et al., 2002). This pattern can be attributed to the steeper slope gradients and shallower soils at hillslope locations compared to terraces, which favour rapid hydrological responses and are consistent with reported rainfall-driven increases in

https://doi.org/10.5194/egusphere-2026-2711
Preprint. Discussion started: 22 May 2026

Q under low antecedent SM (Shen et al., 2025; Zuecco et al., 2016). Thus, the high structural connectivity of these locations likely facilitates the rapid transmission of P inputs toward the outlet before substantial increases in SM are observed.

Despite this responsiveness, the weak SM-Q coupling indicates that local SM dynamics at hillslope locations do not always reflect the integrated microcatchment response. This likely reflects the influence of downslope elements, particularly terraces, which can temporarily store and modulate the transmission of hillslope inputs (McDonnell et al., 2021). Vegetation differences may also contribute, as sparser hillslope vegetation cover can reduce interception and subsurface buffering relative to terraces, potentially enhancing the efficiency of R generation (Jencso and McGlynn, 2011).

4.2.2 Terraces

Terrace locations exhibited contrasting SM-Q relationships depending on their structural position within the hillslope-terrace system. At the high-connectivity upslope-edge terrace, outlet Q was consistently associated with high and relatively constrained SM values across seasons. Compared to hillslopes, this narrower and elevated SM range reflects stronger correspondence between local SM dynamics and outlet Q, indicating closer alignment between local wetness and functional hydrological connectivity toward the outlet. Sharp Q responses at this location suggest storage-controlled connectivity, where local SM must accumulate before lateral transmission becomes effective, particularly under wet conditions (Arnáez et al., 2015; Lei et al., 2020; McDonnell et al., 2021; Moreno-de-las-Heras et al., 2019). P inputs and antecedent SM further modulated these responses (Farrick and Branfireun, 2014; Scaife and Band, 2017), as even modest P inputs can propagate effectively once local SM is sufficiently elevated.

By contrast, the disconnected mid-terrace displayed weak and highly variable SM-Q relationships, particularly during transitional periods, indicating that local SM dynamics at this position were largely decoupled from outlet Q. Only during wet periods did Q occur under a narrower range of higher SM values, consistent with microcatchment-wide spatial hydrological coupling under sustained wet conditions. These more constrained responses may reflect the activation of slower subsurface flow pathways under persistently moist conditions and low atmospheric demand (Detty and McGuire, 2010). SM-Q responses at this site were more diffuse and delayed, requiring longer or more intense P to engage lateral flow, highlighting the role of structural connectivity in guiding hydrological spatial coupling in Mediterranean terraced systems (Arnáez et al., 2015; Calsamiglia et al., 2018).

Vegetation further shaped spatial contrasts across terrace positions. Higher canopy cover and root density enhanced infiltration and transpiration during dry spells, buffering local SM and reducing the likelihood of immediate surface flow activation, whereas sparsely vegetated areas allowed faster R responses (Jencso and McGlynn, 2011). Together with structural connectivity, vegetation regulates how terraces modulate the transmission of hillslope inputs and the emergence of functional connectivity.

https://doi.org/10.5194/egusphere-2026-2711
Preprint. Discussion started: 22 May 2026

Overall, terraces act not merely as passive storage elements but as active modulators of microcatchment-scale hydrological coupling. High-connectivity terrace positions promote strong SM-Q correspondence and efficient lateral flow transmission, while disconnected terrace areas exhibit weak coupling and delayed responses due to combined effects of storage, structural isolation, and vegetation.

4.2.3 Seasonal controls on functional connectivity patterns

Seasonal conditions controlled how spatial patterns of SM-Q relationships were expressed across the hillslope-terrace system, modulating the degree of functional hydrological connectivity between landscape positions. During wet periods, SM conditions associated with outlet Q became more consistent across locations, indicating widespread correspondence between local SM dynamics and outlet response and reflecting broad hydrological coupling across the microcatchment. Under these conditions, monitoring sites approached the range of SM states associated with outlet Q, promoting system-wide connectivity even under moderate P inputs (Farrick and Branfireun, 2014; Penna et al., 2011).

In contrast, during drying-down periods, declining SM reduced functional connectivity and increased spatial heterogeneity in SM-Q relationships. Outlet Q occurred across a wider range of SM conditions, particularly at hillslope and disconnected terrace locations, indicating that the conditions required for R generation became more variable (McNamara et al., 2005; Western et al., 2001). In some cases, outlet Q was observed under relatively low SM, especially at hillslopes, suggesting that rainfall-driven connectivity may be activated independently of local SM conditions (Nanda et al., 2019).

During wetting-up periods, the re-establishment of hydrological coupling was progressive and spatially heterogeneous. More structurally connected locations aligned earlier with outlet Q, while other areas remained decoupled until wetter conditions were reached, reflecting a gradual reactivation of lateral flow pathways (McDonnell et al., 2021). This indicates that functional connectivity recovery is not uniform across the landscape but governed by both antecedent conditions and structural organization.

Vegetation further modulated these seasonal dynamics by influencing SM depletion and recharge. Denser vegetation cover delayed the attainment of wet conditions required for broad hydrological coupling, particularly on terraces, whereas sparsely vegetated hillslopes responded more rapidly to P inputs (Jencso and McGlynn, 2011).

Together, these results demonstrate that functional hydrological connectivity is not only spatially heterogeneous but also seasonally dynamic, with the extent to which local SM dynamics are reflected in Q outlet response depending on the interaction among landscape position, antecedent wetness, atmospheric demand, P inputs and local SM dynamics.

https://doi.org/10.5194/egusphere-2026-2711
Preprint. Discussion started: 22 May 2026

4.3 Implications for hydrological spatial coupling in structurally complex catchments

This study demonstrates that R occurrence in terraced Mediterranean systems emerges from the spatial organization of hydrological coupling, shaped by the interaction between P inputs and SM dynamics across structurally connected and disconnected areas (McDonnell et al., 2021; Turnbull and Wainwright, 2019; Zehe et al., 2007). These findings emphasize the need for modelling approaches that explicitly represent spatial variability in connectivity, hydrological memory, and the transient nature of flow pathways in complex catchments (Nanda and Safeeq, 2023). The event-scale, multi-sensor dataset presented here provides a valuable empirical basis for developing and testing process-based, connectivity-informed hydrological models in the So na Vidala microcatchment and similar environments.

From a land management perspective, terraces and land cover regulate the balance between water storage and transmission, thereby controlling the spatial organization of structural and functional connectivity. Terrace abandonment, degradation, afforestation, or wildfires can alter this balance, reducing connectivity through increased retention and evapotranspiration, or enhancing flow transmission during wet conditions and high-intensity events (Calsamiglia et al., 2018; Moreno-de-las-Heras et al., 2019). Terraced areas with deeper soils and lower structural connectivity can buffer R during moderate events, while steep hillslopes can promote rapid flow transmission under intense P. The unmonitored western sector, characterized by shallow soils and exposed bedrock, likely contributes to fast hydrological responses and may represent an additional source of connectivity to the outlet, despite not being directly monitored due to site constraints.

Vegetation likely represents an additional control on hydrological coupling through its influence on interception, evapotranspiration, and subsurface flow pathways (Assouline et al., 2024; Gallart et al., 2002; Scaife and Band, 2017). Although vegetation effects were not explicitly assessed in this study, spatial heterogeneity in vegetation cover and rooting patterns may further modulate the activation and persistence of functional connectivity across hillslopes and terraces (Jencso and McGlynn, 2011), particularly during transitional seasons. Future work integrating vegetation dynamics with distributed SM and R monitoring could help clarify how ecohydrological processes interact with structural connectivity to regulate R generation under changing climatic and land-use conditions.

Ultimately, these results underscore the importance of long-term, spatially distributed, high-frequency monitoring to capture fine-scale heterogeneity in soil depth, terrain position, vegetation, and anthropogenic structures. Such data are essential not only to improve hydrological understanding but also to inform management strategies that account for spatial and temporal variability in hydrological connectivity, supporting climate resilience, erosion control, and the preservation of cultural landscapes. More broadly, this study shows that hydrological coupling in terraced systems cannot be understood without explicitly considering how structural connectivity constrains and enables functional connectivity across space and time. This perspective provides a unifying framework linking seasonal dynamics, event-scale processes, and spatial variability, and offers

https://doi.org/10.5194/egusphere-2026-2711
Preprint. Discussion started: 22 May 2026

a basis for future connectivity-informed modelling and restoration approaches in Mediterranean catchments under global change.

5 Conclusions

This study investigated temporal and spatial dynamics on R occurrence and hydrological coupling in a structurally complex Mediterranean terraced microcatchment using multi-year P, Q, and distributed SM observations. Outlet R response at So na Vidala was highly episodic, occurring in only ~17 % of P events, with November 2021 alone accounting for 72.9 % of the total R volume. This strong concentration of R in a few events highlights the dominance of non-linear and event-driven hydrological behaviour in Mediterranean headwater systems, being a pattern that can be exacerbated with climate change.

R occurrence was strongly modulated by seasonal variations in SM, which controlled the extent of functional hydrological coupling across the microcatchment. During wet and wetting-up periods, elevated SM promoted widespread connectivity, allowing even moderate P inputs to generate outlet Q. In contrast, during drying-down and dry periods, SM depletion limited connectivity, and R occurrence was restricted to high-magnitude or high-intensity events. These results demonstrate that R generation is governed by state-dependent conditions that vary through time.

At the event-scale, R occurrence reflected the combined influence of P characteristics and SM dynamics. Maximum SM consistently distinguished between flood and non-flow events, while ΔSM provided additional insight into the activation of subsurface connectivity during transitional periods. In contrast, antecedent SM showed limited predictive power overall, indicating that initial wetness alone is insufficient to explain event response without considering within-event SM dynamics.

Marked spatial variability highlighted the role of landscape structure in modulating hydrological coupling. Hillslope locations showed rapid responses to P but weak correspondence between local SM and outlet Q, whereas high-connectivity terrace positions exhibited stronger, storage-controlled behavior. In contrast, the disconnected mid-terrace remained largely decoupled from outlet response except under sustained wet conditions. These differences demonstrate that similar event-scale responses can arise from distinct underlying mechanisms depending on structural connectivity and landscape position.

Overall, R occurrence in Mediterranean terraced microcatchments emerges from the interaction between P forcing and dynamically evolving SM conditions across a spatially heterogeneous landscape. This study highlights the need to explicitly consider spatial variability in connectivity and hydrological coupling when interpreting R generation and developing hydrological models. Such an approach is essential for improving predictions and informing integrated catchment management strategies under changing climatic and land use conditions.

Data availability

https://doi.org/10.5194/egusphere-2026-2711
Preprint. Discussion started: 22 May 2026

Data will be made available on request and will, in due course, be made openly accessible via the Observatory of Natural Risks and Emergencies of the Balearic Islands database (https://riscbal.uib.eu/).

Author contribution

Jaume Company: conceptualization, data curation, formal analysis, investigation, methodology, visualization, writing – original draft preparation. Francisco Cuello-Llobell: conceptualization, data curation, investigation, methodology, writing – review and editing. Julián García-Comendador: conceptualization, data curation, methodology, supervision, writing – review and editing. Josep Fortesa: conceptualization, data curation, methodology, supervision, writing – review and editing. Miquel Tomàs-Burguera: conceptualization, data curation, methodology, supervision, writing – review and editing. Miquel Mir-Gual: conceptualization, data curation, methodology, supervision, validation and writing – review and editing. Laura Turnbull: conceptualization, methodology, supervision, writing – review and editing. John Wainwrigth: conceptualization, methodology, supervision, writing – review and editing. Mariano Moreno-de-las-Heras: conceptualization, methodology, supervision, writing – review and editing. Jordi Cristóbal: conceptualization, data curation, supervision, writing – review and editing. Adolfo Calvo-Cases: conceptualization, writing – review and editing. Joan Estrany: conceptualization, funding acquisition, methodology, project administration, resources, supervision, validation, writing – review and editing.

Competing interests

At least one of the (co-)authors is a member of the editorial board of Hydrology and Earth System Sciences.

Acknowledgments

This work has been sponsored by the research project PID2021-123707OB-I00, "Ecogeomorphic modelling in Mediterranean catchments: multi-scale definition of connectivity thresholds and soil degradation –MEDhyCON3", funded by the Spanish Ministry of Science, Innovation and Universities, the Spanish Research Agency (AEI), and the European Regional Development Funds (ERDF); and "Floods and Droughts – GenAI-enabled solutions for water resilience and citizen-centered crisis management-101299010", supported by the Digital Europe Programme (2021-2027). Jaume Company is in receipt of a predoctoral contract [FPI-UIB] from the University of the Balearic Islands, funded by the ERDF. Francisco Cuello-Llobell is in receipt of a predoctoral contract [PRE2022-101607] funded by the Spanish Ministry of Science, Innovation and Universities. During the preparation of this work, the author(s) used ChatGPT (OpenAI, 2025) to support English language editing and improve clarity in the manuscript.

https://doi.org/10.5194/egusphere-2026-2711
Preprint. Discussion started: 22 May 2026

References

Abatzoglou, J. T., Williams, A. P., and Barbero, R.: Global Emergence of Anthropogenic Climate Change in Fire Weather Indices, Geophys. Res. Lett., 46, 326–336, https://doi.org/10.1029/2018GL080959, 2019.

Allen, R. G., Pereira, L. S., Raes, D., and Smith, M.: Crop evapotranspiration-Guidelines for computing crop water requirements-FAO Irrigation and drainage paper 56, Fao, rome, 300, D05109, 1998.

Arnáez, J., Lana-Renault, N., Lasanta, T., Ruiz-Flaño, P., and Castroviejo, J.: Effects of farming terraces on hydrological and geomorphological processes. A review, https://doi.org/10.1016/j.catena.2015.01.021, 1 May 2015.

Assouline, S., Sela, S., Dorman, M., and Svoray, T.: Runoff generation in a semiarid environment: The role of rainstorm intra-event temporal variability and antecedent soil moisture, Adv. Water Resour., 188, 104715, https://doi.org/10.1016/j.advwatres.2024.104715, 2024.

Blume, T., Zehe, E., and Bronstert, A.: Use of soil moisture dynamics and patterns at different spatio-temporal scales for the investigation of subsurface flow processes, Hydrol. Earth Syst. Sci., 13, 1215–1234, https://doi.org/10.5194/hess-13-1215-2009, 2009.

Bracken, L. J., Wainwright, J., Ali, G. A., Tetzlaff, D., Smith, M. W., Reaney, S. M., and Roy, A. G.: Concepts of hydrological connectivity: Research approaches, Pathways and future agendas, https://doi.org/10.1016/j.earscirev.2013.02.001, 1 April 2013.

Buttle, J. M., Dillon, P. J., and Eerkes, G. R.: Hydrologic coupling of slopes, riparian zones and streams: An example from the Canadian Shield, J. Hydrol. (Amst)., 287, 161–177, https://doi.org/10.1016/j.jhydrol.2003.09.022, 2004.

Calsamiglia, A., Lucas-Borja, M. E., Fortesa, J., García-Comendador, J., and Estrany, J.: Changes in soil quality and hydrological connectivity caused by the abandonment of terraces in a Mediterranean burned catchment, Forests, 8, https://doi.org/10.3390/f8090333, 2017.

Calsamiglia, A., Fortesa, J., García-Comendador, J., Lucas-Borja, M. E., Calvo-Cases, A., and Estrany, J.: Spatial patterns of sediment connectivity in terraced lands: Anthropogenic controls of catchment sensitivity, Land Degrad. Dev., 29, 1198–1210, https://doi.org/10.1002/ldr.2840, 2018.

Calvo-Cases, A., Arnau-Rosalén, E., Boix-Fayos, C., Estrany, J., Roxo, M. J., and Symeonakis, E.: Eco-geomorphological connectivity and coupling interactions at hillslope scale in drylands: Concepts and critical examples, J. Arid Environ., 186, 104418, https://doi.org/10.1016/j.jaridenv.2020.104418, 2021.

Certini, G.: Effects of fire on properties of forest soils: A review, https://doi.org/10.1007/s00442-004-1788-8, 2 March 2005.

Crema, S. and Cavalli, M.: SedInConnect: a stand-alone, free and open source tool for the assessment of sediment connectivity, Comput. Geosci., 111, 39–45, https://doi.org/10.1016/j.cageo.2017.10.009, 2018.

Detty, J. M. and McGuire, K. J.: Topographic controls on shallow groundwater dynamics: Implications of hydrologic connectivity between hillslopes and riparian zones in a till mantled catchment, Hydrol. Process., 24, 2222–2236, https://doi.org/10.1002/hyp.7656, 2010.

https://doi.org/10.5194/egusphere-2026-2711
Preprint. Discussion started: 22 May 2026

Dymond, S. F., Wagenbrenner, J. W., Keppeler, E. T., and Bladon, K. D.: Dynamic Hillslope Soil Moisture in a Mediterranean Montane Watershed, Water Resour. Res., 57, e2020WR029170, https://doi.org/10.1029/2020WR029170, 2021.

Estrany, J., Ruiz, M., Calsamiglia, A., Carriquí, M., García-Comendador, J., Nadal, M., Fortesa, J., López-Tarazón, J. A., Medrano, H., and Gago, J.: Sediment connectivity linked to vegetation using UAVs: High-resolution imagery for ecosystem management, Science of the Total Environment, 671, 1192–1205, https://doi.org/10.1016/j.scitotenv.2019.03.399, 2019.

Farrick, K. K. and Branfireun, B. A.: Soil water storage, rainfall and runoff relationships in a tropical dry forest catchment, Water Resour. Res., 50, 9236–9250, https://doi.org/10.1002/2014WR016045, 2014.

Fortesa, J., Latron, J., García-Comendador, J., Company, J., and Estrany, J.: Runoff and soil moisture as driving factors in suspended sediment transport of a small mid-mountain Mediterranean catchment, Geomorphology, 368, 107349, https://doi.org/10.1016/j.geomorph.2020.107349, 2020.

Gallart, F., Llorens, P., and Latron, J.: Studying the role of old agricultural terraces on runoff generation in a small Mediterranean mountainous basin, J. Hydrol. (Amst)., 159, 291–303, https://doi.org/10.1016/0022-1694(94)90262-3, 1994.

Gallart, F., Llorens, P., Latron, J., and Regüés, D.: Hydrological processes and their seasonal controls in a small Mediterranean mountain catchment in the Pyrenees, Hydrol. Earth Syst. Sci., 6, 527–537, https://doi.org/10.5194/hess-6-527-2002, 2002.

García-Comendador, J., Fortesa, J., Calsamiglia, A., Calvo-Cases, A., and Estrany, J.: Post-fire hydrological response and suspended sediment transport of a terraced Mediterranean catchment, Earth Surf. Process. Landf., 42, 2254–2265, https://doi.org/10.1002/esp.4181, 2017.

Garcia-Estringana, P., Latron, J., Llorens, P., and Gallart, F.: Spatial and temporal dynamics of soil moisture in a Mediterranean mountain area (Vallcebre, NE Spain), Ecohydrology, 6, 741–753, https://doi.org/10.1002/eco.1295, 2013.

Grayson, R. B., Western, A. W., Chiew, F. H. S., and Blöschl, G.: Preferred states in spatial soil moisture patterns: Local and nonlocal controls, in: Water Resources Research, 2897–2908, https://doi.org/10.1029/97WR02174, 1997.

Jencso, K. G. and McGlynn, B. L.: Hierarchical controls on runoff generation: Topographically driven hydrologic connectivity, geology, and vegetation, Water Resour. Res., 47, 11527, https://doi.org/10.1029/2011WR010666, 2011.

Jones, M. W., Abatzoglou, J. T., Veraverbeke, S., Andela, N., Lasslop, G., Forkel, M., Smith, A. J. P., Burton, C., Betts, R. A., van der Werf, G. R., Sitch, S., Canadell, J. G., Santín, C., Kolden, C., Doerr, S. H., and Le Quéré, C.: Global and Regional Trends and Drivers of Fire Under Climate Change, https://doi.org/10.1029/2020RG000726, 1 July 2022.

Kaffas, K., Murgia, I., Menapace, A., Macchioli Grande, M., Verdone, M., Dani, A., Manca di Villahermosa, F. S., Preti, F., Segura, C., Massari, C., Klaus, J., Borga, M., and Penna, D.: Controls on preferential flow and its role on streamflow generation in a Mediterranean forested catchment, J. Hydrol. (Amst)., 660, 133469, https://doi.org/10.1016/j.jhydrol.2025.133469, 2025.

Keller, Z. T., Vivoni, E. R., Kimsal, C. R., Robles-Morua, A., and Pérez-Ruiz, E. R.: Hillslope to channel hydrologic connectivity in a dryland ecosystem, Ecosphere, 14, e4707, https://doi.org/10.1002/ECS2.4707, 2023.

Latron, J. and Gallart, F.: Seasonal dynamics of runoff-contributing areas in a small mediterranean research catchment (Vallcebre, Eastern Pyrenees), J. Hydrol. (Amst)., 335, 194–206, https://doi.org/10.1016/j.jhydrol.2006.11.012, 2007.

https://doi.org/10.5194/egusphere-2026-2711
Preprint. Discussion started: 22 May 2026

Latron, J. and Gallart, F.: Runoff generation processes in a small Mediterranean research catchment (Vallcebre, Eastern Pyrenees), J. Hydrol. (Amst)., 358, 206–220, https://doi.org/10.1016/j.jhydrol.2008.06.014, 2008.

Latron, J., Soler, M., Llorens, P., and Gallart, F.: Spatial and temporal variability of the hydrological response in a small Mediterranean research catchment (Vallcebre, Eastern Pyrenees), Hydrol. Process., 22, 775–787, https://doi.org/10.1002/hyp.6648, 2008.

Lei, W., Dong, H., Chen, P., Lv, H., Fan, L., and Mei, G.: Study on Runoff and Infiltration for Expansive Soil Slopes in Simulated Rainfall, Water (Switzerland), 12, 222, https://doi.org/10.3390/w12010222, 2020.

Licciardello, F., Barbagallo, S., and Gallart, F.: Hydrological and erosional response of a small catchment in Sicily, Journal of Hydrology and Hydromechanics, 67, 201–212, https://doi.org/10.2478/johh-2019-0003, 2019.

Llorens, P., Gallart, F., Cayuela, C., Roig-Planasdemunt, M., Casellas, E., Molina, A. J., Moreno De Las Heras, M., Bertran, G., Sánchez-Costa, E., and Latron, J.: What have we learnt about mediterranean catchment hydrology? 30 years observing hydrological processes in the Vallcebre research catchments, Geographical Research Letters, 44, 475–502, https://doi.org/10.18172/cig.3432, 2018.

Lucas-Borja, M. E., Calsamiglia, A., Fortesa, J., García-Comendador, J., Lozano Guardiola, E., García-Orenes, F., Gago, J., and Estrany, J.: The role of wildfire on soil quality in abandoned terraces of three Mediterranean micro-catchments, Catena (Amst)., 170, 246–256, https://doi.org/10.1016/j.catena.2018.06.014, 2018.

Masselink, R. J. H., Heckmann, T., Temme, A. J. A. M., Anders, N. S., Gooren, H. P. A., and Keesstra, S. D.: A network theory approach for a better understanding of overland flow connectivity, Hydrol. Process., 31, 207–220, https://doi.org/10.1002/hyp.10993, 2017.

McDonnell, J. J., Spence, C., Karran, D. J., van Meerveld, H. J., and Harman, C. J.: Fill-and-Spill: A Process Description of Runoff Generation at the Scale of the Beholder, https://doi.org/10.1029/2020WR027514, 1 May 2021.

McNamara, J. P., Chandler, D., Seyfried, M., and Achet, S.: Soil moisture states, lateral flow, and streamflow generation in a semi-arid, snowmelt-driven catchment, Hydrol. Process., 19, 4023–4038, https://doi.org/10.1002/hyp.5869, 2005.

Merz, B. and Plate, E. J.: An analysis of the effects of spatial variability of soil and soil moisture on runoff, in: Water Resources Research, 2909–2922, https://doi.org/10.1029/97WR02204, 1997.

Moreno-de-las-Heras, M., Lindenberger, F., Latron, J., Lana-Renault, N., Llorens, P., Arnáez, J., Romero-Díaz, A., and Gallart, F.: Hydro-geomorphological consequences of the abandonment of agricultural terraces in the Mediterranean region: Key controlling factors and landscape stability patterns, https://doi.org/10.1016/j.geomorph.2019.02.014, 15 May 2019.

Nanda, A. and Safeeq, M.: Threshold controlling runoff generation mechanisms in Mediterranean headwater catchments, J. Hydrol. (Amst)., 620, 129532, https://doi.org/10.1016/j.jhydrol.2023.129532, 2023.

Nanda, A., Sen, S., and McNamara, J. P.: How spatiotemporal variation of soil moisture can explain hydrological connectivity of infiltration-excess dominated hillslope: Observations from lesser Himalayan landscape, J. Hydrol. (Amst)., 579, 124146, https://doi.org/10.1016/j.jhydrol.2019.124146, 2019.

https://doi.org/10.5194/egusphere-2026-2711
Preprint. Discussion started: 22 May 2026

Nippgen, F., McGlynn, B. L., and Emanuel, R. E.: The spatial and temporal evolution of contributing areas, Water Resour. Res., 51, 4550–4573, https://doi.org/10.1002/2014WR016719, 2015.

Penna, D., Tromp-Van Meerveld, H. J., Gobbi, A., Borga, M., and Dalla Fontana, G.: The influence of soil moisture on threshold runoff generation processes in an alpine headwater catchment, Hydrol. Earth Syst. Sci., 15, 689–702, https://doi.org/10.5194/hess-15-689-2011, 2011.

Preti, F., Guastini, E., Penna, D., Dani, A., Cassiani, G., Boaga, J., Deiana, R., Romano, N., Nasta, P., Palladino, M., Errico, A., Giambastiani, Y., Trucchi, P., and Tarolli, P.: Conceptualization of Water Flow Pathways in Agricultural Terraced Landscapes, Land Degrad. Dev., 29, 651–662, https://doi.org/10.1002/ldr.2764, 2018.

Saffarpour, S., Western, A. W., Adams, R., and McDonnell, J. J.: Multiple runoff processes and multiple thresholds control agricultural runoff generation, Hydrol. Earth Syst. Sci., 20, 4525–4545, https://doi.org/10.5194/hess-20-4525-2016, 2016.

Scaife, C. I. and Band, L. E.: Nonstationarity in threshold response of stormflow in southern Appalachian headwater catchments, Water Resour. Res., 53, 6579–6596, https://doi.org/10.1002/2017WR020376, 2017.

Shakesby, R. A.: Post-wildfire soil erosion in the Mediterranean: Review and future research directions, https://doi.org/10.1016/j.earscirev.2011.01.001, April 2011.

Shen, Q., Zhang, Y., Yan, Y., Dong, H., and Lei, W.: Experimental Study on Infiltration Characteristics of Shallow Rainwater in Expansive Soil Slopes at Different Gradients, Water (Switzerland), 17, https://doi.org/10.3390/w17050642, 2025.

Singh, N. K., Emanuel, R. E., McGlynn, B. L., and Miniat, C. F.: Soil Moisture Responses to Rainfall: Implications for Runoff Generation, Water Resour. Res., 57, e2020WR028827, https://doi.org/10.1029/2020WR028827, 2021.

Srinivasan, M. S., Gburek, W. J., and Hamlett, J. M.: Dynamics of stormflow generation-A hillslope-scale field study in East-Central Pennsylvania, USA, Hydrol. Process., 16, 649–665, https://doi.org/10.1002/hyp.311, 2002.

Soil Survey Staff: Soil taxonomy: A basic system of soil classification for making and interpreting soil surveys, 2nd Editio., edited by: Handbook, U. S. D. of A., Natural Resources Conservation Service, 1999.

Tromp-Van Meerveld, H. J. and McDonnell, J. J.: Threshold relations in subsurface stormflow: 2. The fill and spill hypothesis, Water Resour. Res., 42, 2411, https://doi.org/10.1029/2004WR003800, 2006.

Turnbull, L. and Wainwright, J.: From structure to function: Understanding shrub encroachment in drylands using hydrological and sediment connectivity, Ecol. Indic., 98, 608–618, https://doi.org/10.1016/j.ecolind.2018.11.039, 2019.

Turnbull, L., Wainwright, J., and Brazier, R. E.: A conceptual framework for understanding semi-arid land degradation: ecohydrological interactions across multiple-space and time scales, Ecohydrology, 1, 23–34, https://doi.org/10.1002/ECO.4, 2008.

Wainwright, J.: Degrees of separation: Hillslope-channel coupling and the limits of palaeohydrological reconstruction, Catena (Amst)., 66, 93–106, https://doi.org/10.1016/j.catena.2005.07.016, 2006.

Wainwright, J., Turnbull, L., Ibrahim, T. G., Lexartza-Artza, I., Thornton, S. F., and Brazier, R. E.: Linking environmental régimes, space and time: Interpretations of structural and functional connectivity, Geomorphology, 126, 387–404, https://doi.org/10.1016/j.geomorph.2010.07.027, 2011.

https://doi.org/10.5194/egusphere-2026-2711
Preprint. Discussion started: 22 May 2026

Western, A. W., Blöschl, G., and Grayson, R. B.: Toward capturing hydrologically significant connectivity in spatial patterns, Water Resour. Res., 37, 83–97, https://doi.org/10.1029/2000WR900241, 2001.

Xiong, J. and Yang, Y.: Climate Change and Hydrological Extremes, Current Climate Change Reports 2024 11:1, 11, 1-, https://doi.org/10.1007/S40641-024-00198-4, 2024.

Zehe, E., Elsenbeer, H., Lindenmaier, F., Schulz, K., and Blöschl, G.: Patterns of predictability in hydrological threshold systems, Water Resour. Res., 43, https://doi.org/10.1029/2006WR005589, 2007.

Zhang, Y., Wei, H., and Nearing, M. A.: Effects of antecedent soil moisture on runoff modeling in small semiarid watersheds of southeastern Arizona, Hydrol. Earth Syst. Sci., 15, 3171–3179, https://doi.org/10.5194/hess-15-3171-2011, 2011.

Zuecco, G., Penna, D., Borga, M., and van Meerveld, H. J.: A versatile index to characterize hysteresis between hydrological variables at the runoff event timescale, Hydrol. Process., 30, 1449–1466, https://doi.org/10.1002/hyp.10681, 2016.